Université de Montréal

Study of Thermosensitive Microspheres for Potential Applications in Biosensing

Par

Yilong Chen

Département de chimie

Faculté des arts et des sciences

Mémoire présenté à la faculté des études supérieures en vue de l'obtention du grade de maîtrise en chimie

Août 2006

Université de Montréal
Faculté des études supérieures

Ce mémoire intitulé

Study of Thermosensitive Microspheres for Potential Applications in Biosensing

Présenté par
Yilong Chen

A été évalué par un jury composé des personnes suivantes:

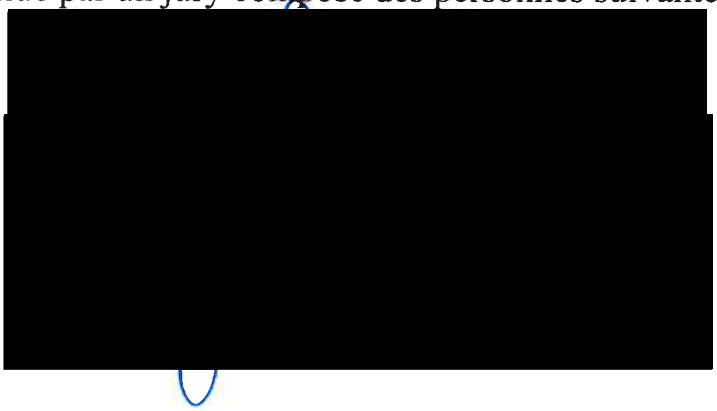

Résumé

En contrôlant le ratio tensioactif/monomère, des particules de microgel thermosensible de différentes tailles ont été synthétisées par polymérisation en émulsion. Nous avons observé qu'un arrangement colloïdal cristallin se forme lors de variations contrôlées de température. Certaines de ces particules ont été enduites d'une couche de polymère réticulé non-thermosensible de poly(acrylamide) et de poly(*N*,*N*-diméthyl acrylamide) ou thermosensible de poly(*N*,*N*-diéthyl acrylamide) et de poly(*N*-isopropyl acrylamide) afin d'obtenir une ou deux températures de transition dans le réseau colloïdal cristallin. En utilisant la théorie de Flory, les phénomènes de diffraction et de gonflement peuvent être expliqués en termes des énergies de mélange et élastique. L'influence sur la diffraction du changement de pH et de la force ionique du milieu a été étudiée afin d'évaluer le potentiel de ces matériaux comme capteurs.

Des microsphères conchoïdales (avec noyaux centraux) ont aussi été synthétisées. Ces microsphères sont constituées d'un noyau chimiquement réticulé et d'une enveloppe 'chevelue'. Le noyau est formé de poly(*N*-isopropyl acrylamide-*co*-styrène) alors que la couche externe est formée de poly(*N*,*N*-diéthyl acrylamide), de poly(*N*-isopropyl acrylamide) ou de poly(*N*-isopropyl methacrylamide). Grâce à la microscopie électronique à transmission et à la diffusion dynamique de la lumière, le gonflement et la morphologie de ces microsphères ont pu être étudiés. Celles portant une couche de polymère thermosensible présentent une contraction (rétricissement) en deux étapes avec la température.

Par la formation de liaisons covalentes entre la biotine et les particules thermosensibles, une étude par spectroscopie de fluorescence des interactions avec l'avidine et la streptavidine démontre une réponse suffisante pour envisager des applications comme biocapteurs.

Mots-clés: Cristal colloïdal; Microgel; Diffusion de la lumière; Particule; Biotine-avidine; Capteurs.

ABSTRACT

Thermosensitive microgel particles were synthesized via emulsion polymerization and the in size was controlled by varying the concentrations of monomers and surfactant. The thermo-responsive and soft particles formed colloidal crystalline array (CCA) through a simple temperature cycling procedure. The CCAs were embedded in both cross-linked nonthermosensitive matrices of polyacrylamide and poly(*N*,*N*-dimethyl acrylamide) and thermosensitive poly(*N*,*N*-diethyl acrylamide) and poly(*N*-isopropyl acrylamide) to fabricate films of polymerized colloidal crystalline arrays (PCCAs) with single and doubly thermosensitivities, respectively. Their temperature dependent diffraction behavior was investigated to reveal the swelling properties of the gels, which were interpreted by classical Flory's polymer theories. The combination of mixing and elastic energies affected the swelling properties of polymerized colloidal crystalline arrays. Finally, ionic strength and pH effects on the CCA diffraction behavior were studied.

These core-shell microspheres are composed of chemically cross-linked poly(*N*-propyl acrylamide-*co*-styrene) with different styrene contents as a core and hairy poly(*N*,*N*-diethyl acrylamide), poly(*N*-isopropyl acrylamide) and poly(*N*-isopropyl methacrylamide) as shells. The morphologies and swelling properties of the core and core-shell microspheres were investigated by means of transmission electron microscopy, optical transmission and dynamic light scattering. The core-shell microspheres display a temperature-dependent two-step shrinking behavior.

The thermosensitive microgel particles were biotinylated and their interactions with avidin and streptavidin were studied by fluorescence spectroscopies. The results showed that the microgel particles could respond to the presence of avidin or streptavidin, which may have potential applications as biosensors.

Keywords: Colloidal crystal; Microgel; Light diffraction; Particle; Biotin-avidin; Sensor.

TABLE OF CONTENTS

LIST OF FIGURES

LIST OF TABLES

LIST OF SYMBOLS AND ABBREVIATIONS

AAm	Acrylamide
BA	*N*,*N'*-Methylenebisacrylamide
CCA	Colloidal crystalline array
DEA	*N*,*N*-Diethylacrylamide
DEAP	Diethoxyacetophenone
DMA	*N*,*N*-Dimethylacrylamide
d	Interplanar spacing
EA	*N*-Ethylacrylamide
ΔG_E	Elastic free energy change
ΔG_{ion}	Ionization free energy change
ΔG_m	Mixing free energy change
HEMA	2-Hydroxyethyl methacrylate
k	Boltzmann constant
K_d	Dissociation constant
KPS	Potassium persulfate
LCST	Lower critical solution temperature
m	Order of diffraction
n	Refractive index
NAS	*N*-Acryloxysuccinimide
NIPAM	*N*-Isopropylacrylamide
NIPMAM	*N*-Isopropyl methacrylamide
nPA	*N*-n-Propyl acrylamide
PCCA	Polymerized colloidal crystalline array
R_h	Hydrodynamic diameter
S	Styrene
SDS	Sodium dodecyl sulfate
T	Absolute temperature
$t_{1/2}$	Half life
UCST	Upper critical solution temperature
V	Volume of the gel

V_{H_2O}	Molar volume of water
V_m	Volume of the fully relaxed gel
VPT	Volume phase transition
δ_{H_2O}	Solubility parameter of water
$\overline{\delta}_P$	Average solubility parameter of the polymer
ε	Absorbance coefficient
θ	Glancing angle
λ	Diffraction wavelength of PCCA films
λ_0	Diffraction wavelength of dry PCCA films
λ_m	Diffraction wavelength of relaxed PCCA films
τ	Fluorescence lifetime
ν_e/V_m	Cross-linking density
ϕ	Polymer volume fraction
ϕ_{eff}	Effective volume fraction
χ	Flory-Huggins polymer/solvent interaction parameter

ACKNOWLEDGEMENTS

This thesis is by far the most significant scientific accomplishment in my life and it would have been impossible to complete without the people who supported me and believed in me.

Most of all I would like to thank my research supervisor, Professor Julian X.X. Zhu of the Department of Chemistry at Université de Montréal. He is not only a great scientist but also a kind person. His trust and scientific rigor inspired me in the most important moments of making right decisions and I am glad to have worked with him.

I wish to thank sincerely Dr. Julien E. Gautrot for his kind help with the correction of the papers in this thesis.

I am also very grateful to Dr. Zhanyong Li of the Institute of Polymer Chemistry at Nankai University for helping me with the PCCA syntheses and discussion.

I want to thank all of the nice friends in the group: Dr. Mathilde Colonne, Dr. Sophie Tan, Marc Gauthier, Héloïse Thérien-Aubin, Dr. Huiyou Liu, Dr. Wilms Baille, Shanshan Chen, Dr. Junhua Zhang, Dr. Juntao Luo, Guillaume Giguère, Claire Jaubert, Bao Toan Nguyen, Fansheng Meng, Julie Boivin, Dr. Ya Cao, Sen Ge, Florence Janvier, Cindy Charboneau, Gérald Perron, Dr. Steven Holden…

My family has provided the spiritual support that is even more important. I thank my parents Zuqi Chen and Aixiang Ding, and my girlfriend Guiying Tang.

1. General Introduction

1.1. Stimuli-responsive polymers

Stimuli-responsive polymers have been investigated extensively for the development of "smart" materials for their potential applications in the controlled transport and delivery of active substances, such as drugs, in biotechnology, medicine, pharmacy or cosmetics.[1] The term 'stimuli-responsive' implies remarkable changes of certain properties induced by an external stimulus. In the strict sense, the induced property changes should be reversible if the stimulus is suppressed or released, or if a second 'reverse' stimulus is applied. Many types of stimuli are theoretically useful, but the choice is limited for practical reasons. In aqueous systems, stimuli-sensitive systems are generally aimed to change the hydrophilic character of a functional group to a hydrophobic one, or vice versa.[2] Both chemical and physical stimuli (which may be coupled) can be employed for this purpose. Chemical stimuli include for instance acid-base reactions, complexation, redox, electrochemical reactions, and photochemical reactions. Physical stimuli comprise changes in pH-value, ionic strength, temperature, pressure, light, and electrical or magnetic fields.[3] Photochemical reactions and redox reactions have also been considered alternatively for applications as switches in aqueous media.[4-14] However, good stability and reversibility in combination with marked changes of the hydrophilic-hydrophobic balance are hard to achieve simultaneously. Particularly, most organic redox systems are chemically sensitive to oxygen from air or to good nucleophiles (like water) in one of the two oxidation states, thus hampering their applications severely. Due to the lack of stability and reversibility, the research interest has moved to the simplest systems driven by pH and temperature.

1.1.1. pH-sensitive polymers

One of the simplest stimuli-responsive polymers is based on acid-base reactions or on pH changes. Typical examples are polymeric amines or polymeric carboxylic acids, which by protonation/deprotonation become charged or neutral, and thus undergo a pronounced change in their hydrophilicity or hydrophobicity. Poly(4-vinyl pyridine),

poly(2-vinyl pyridine), poly(acrylic acid), and poly(methacrylic acid) and their copolymers, are well-known polymers that can respond to a pH change.[15-17] For example, poly(4-vinyl pyridine) swells upon a decrease in pH since the protonation of the pyridinyl groups along the polymer chain leads to increased solubility of the polymer and repulsive electrostatic forces within the particle (Figure 1.1A). The polymer chain collapses upon deprotonation at high pH values. In contrast, polymers made of (meth)acrylic acid can respond to changes in pH and ionic strength, e.g., at pH values below 4, precipitation occurs in aqueous solutions due to the protonation of the carboxylate groups (Figure 1.1B), which renders the polymers sparsely soluble in water.

Such pH-responsive polymers have an excellent reversibility but only for a few switching cycles. Salt accumulation while changing the pH (addition of acid or base) increases the ionic strength of the solution, which can reduce the reversibility and solubility of the pH-responsive polymers.[15-17] Salt accumulation during successive protonation/deprotonation events can render the polymers insoluble in the system.

1.1.2. Thermosensitive polymers

Thermosensitive polymers may exhibit a change in solubility upon changes in temperature. They often possess an upper critical solution temperature (UCST) or a lower critical solution temperature (LCST) depending on their chemical structures. There are a few reports concerning polymers exhibiting a property change on UCST in aqueous solutions.[18-20] Among polymers showing UCST, poly(*N*-acetylacrylamide), containing the *N*-substituted acetyl group, is a representative polymer by exhibiting reversible solubility changes in aqueous solution when heating-up and cooling-down. The hydrogel prepared from the UCST polymer is known to swell while heated above the UCST (Figure 1.2A).[18] It is speculated that an interpolymer complex formed by the mutual association between molecules of the UCST polymer dissociates and turns soluble with hydration in the heating process. Additives might participate in the dissociation between polymer chains to change the UCST. Some kinds of interpolymer complexes were studied by using viscometry and optical measurements.[21-23] However, the effect of additives on the UCST polymer in aqueous system has not been studied

widely so far.

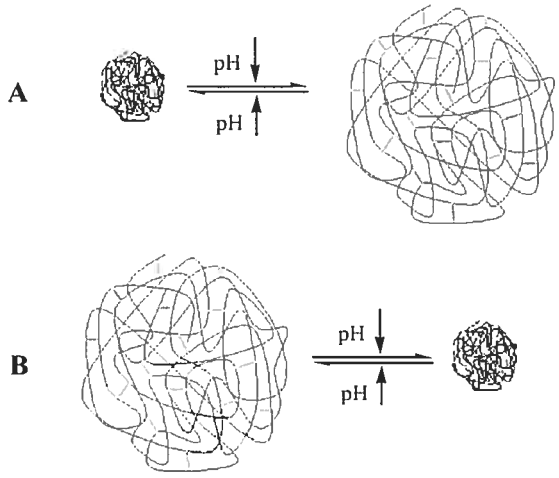

Figure 1.1. pH response of (A) poly(2-vinyl pyridine) and (B) poly(acrylic acid).

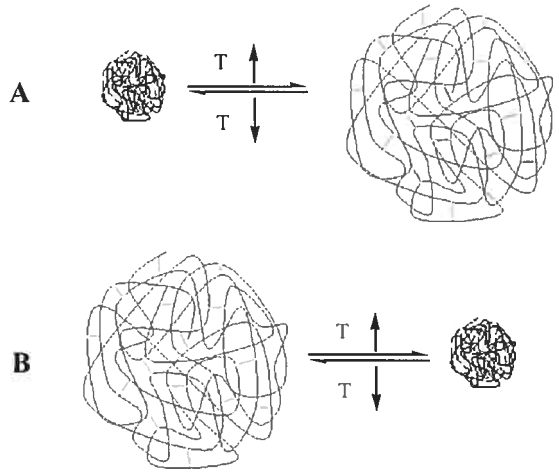

Figure 1.2. Temperature response of (A) UCST polymer particles and (B) LCST polymer particles.

The thermal properties of polymers with a LCST have been investigated extensively.[24-26] These polymers possess both hydrophobic and hydrophilic groups. The balance between hydrophobicity and hydrophilicity determines the LCST properties. These polymers are soluble or swellable below the LCST due to hydrogen bonding in aqueous medium, while the hydrogen bonds are broken by heating above LCST leading

to the precipitation or shrinkage of the polymers in aqueous solutions (Figure 1.2B). *N*-Alkyl substituted polyacrylamide and polymethacrylamide are typical examples of polymers having a LCST (Table 1.1).[24-26] Poly(*N*-isopropylacrylamide) (PNIPAM) is representative of this family of polymers and has been studied for many potential applications in the fields of drug delivery,[27-30] biosensing,[31,32] chemical separations,[33-35] biomaterials,[36-38] and catalysis.[39-41]

Table 1.1. LCST of aqueous solution of *N*-alkyl substituted polyacrylamide (PAAm) and polymethacrylamide (PMAm) (copied and modified from original in ref. 25).

R^1	R^2	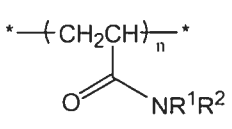	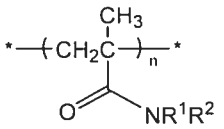
		°C	°C
H	H	—	—
H	CH_3	—	—
CH_3	CH_3	—	—
H	CH_2CH_3	73	—
CH_3	C_2H_5	56-57	—
	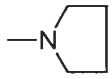	56	—
	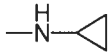	47	—
C_2H_5	C_2H_5	36	—
H	$CH(CH_3)_2$	32	45
CH_3	$CH(CH_3)_2$	25	—
H	$CH_2CH_2CH_3$	22	28
CH_3	$CH_2CH_2CH_3$	15	—
	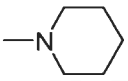	—	—

1.2. Colloidal crystalline arrays (CCA)

There is much interest in the use of photonic crystals to control the propagation of electromagnetic radiation. The self-assembly of three-dimentional (3-D) CCA is a process of broad interests due to its applicability in many fields, such as the study of condensed matter phase behaviors,[42-45] the fabrication of mesoporous films,[46,47] and the development of photonic materials.[48-58] These CCAs diffract light and prevent its transmission following the Bragg's law in a similar way to X-ray diffraction by atomic crystals. These properties have been applied to the fabrication of chemical and biological sensors,[53] optical waveguides,[59] optical switches,[51] and optical filters.[58]

3D-photonic crystals based on materials such as silica, polystyrene (PS), or poly(methyl methacrylate) particles were studied extensively, using sedimentation or particle repulsion to generate ordered structures. These techniques typically rely on nonspecific particle-particle repulsion, which could be short or long range repulsion forces, to induce order. For short-range repulsion forces (hard sphere interactions), close-packed crystalline arrays are typically formed. For example, close packing can be accomplished through slow particle sedimentation, centrifugation, spin coating, electrophoretic deposition, sonication, and lateral compression of interface-bound monolayers. Because close-packed ordered structure typically involves the concentration of particles in a confined space, these studies often involve hard spheres that undergo little deformation upon packing (Figure 1.3).[60,61] Long-range interactions can be exploited to create ordered assemblies. Specifically, suspended colloidal spheres bearing high surface charge densities spontaneously assemble into solvated crystalline arrays when the solution is rigorously desalted (Figure 1.4). These methods, coupled to the photopolymerization of a monomer solution surrounding the CCA, have been exploited by Asher and co-workers to create polymerized colloidal crystalline arrays (PCCA) for optical filtering, switching, and sensing applications.[51-53] However, the thermosensitive amphiphilic soft hydrogel microspheres cannot be ordered by using such approaches, since these particles are too buoyant in water to sediment at an appreciable rate. Filtration or slow evaporation methods are equally inappropriate because of the extreme solvation of the particles, which would collapse upon solvent

removal. Lyon and co-workers have demonstrated that lightly cross-linking hydrogel PNIPAM could form colloidal crystalline arrays through concentration by centrifugation.[55-57] Their results showed that as the effective volume fraction of the microgel crystals (ϕ_{eff}) was decreased by reducing the polymer concentration, the lattice constant increased and the crystals eventually melted into a fluid phase at $\phi_{eff} = 0.49$. When the temperature was raised above the LCST for the component particles, the effective volume fraction became remarkably small as well and the array became a milky-white, disordered, and free-flowing solution (Figure 1.5). They suggested that particles were compressed together to form crystalline arrays by studying the light diffraction behaviors of samples centrifuged at different temperatures and by differential interference contrast microscopy.

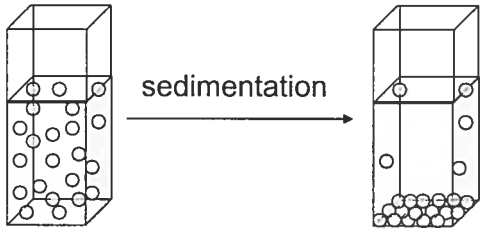

Figure 1.3. Assembly of hard particles by slow particle sedimentation.

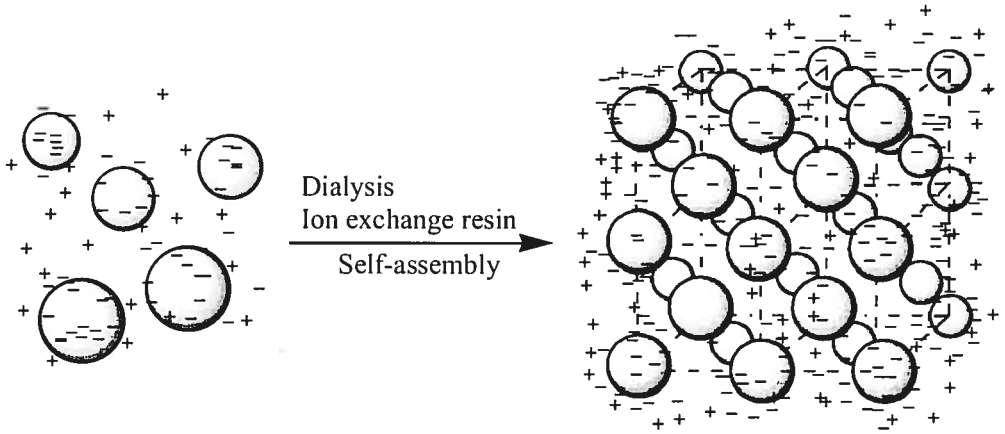

Figure 1.4. Assembly of charged polystyrene (PS) by electrostatic repulsion (copied and modified from original in ref. 51).

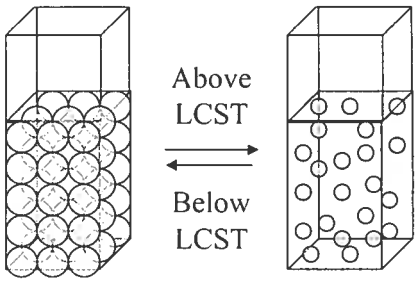

Figure 1.5. Assembly of lightly cross-linked, thermosensitive, uncharged and soft particles.

1.3. Polymerized CCA (PCCA)

It is well-known that the self-assembly of monodispersed charged particles, such as PS,[51,53,62] PNIPAM,[52] and poly(methyl methacrylate)[44] produces three dimensionally periodic structures. This phenomenon is primarily due to the electrostatic interactions of charges at the surface of the particles, coupled to the diffuse counterion cloud (Figure 1.4). If a monomer solution surrounding the CCA is photopolymerized (Figure 1.6), a PCCA is generated, as has been reported by Asher and co-workers for use in optical filtering, switching, and sensing applications.[51-53,62] When charged poly(styrene-*co*-styrene sulfonate) CCAs were embedded in PNIPAM matrix, the periodic lattice was found to change with temperature, while PCCAs fabricated in a PAAm matrix did not show such a phenomenon. Recently, it was found that lightly cross-linked thermosensitive particles, displaying LCSTs, could form CCAs spontaneously via a simple temperature cycling process.[55-57,63,64] The CCAs formed diffracted a wide range of wavelengths, depending on the concentration and the sizes of the particles. However, such "soft" CCA lattices are relatively unstable. For instance, heating the sample above its LCST quantitatively breaks the ordered lattice and so does dilution. Therefore, it appears that PCCAs possess much better thermal, chemical and mechanical stability than CCAs, as demonstrated by Hu's work on PCCA films.[64] However, the control of the CCA ordered structure during the matrix formation step remains an issue, especially in the case of soft CCAs. Lyon and co-workers studied the behaviors of microcomposite

hydrogel films composed of lightly cross-linked PNIPAM particles and PNIPAM matrix.[63] However, they could not preserve the ordered structure of the CCAs upon photopolymerization and the PCCAs they obtained did not show any opalescent properties.

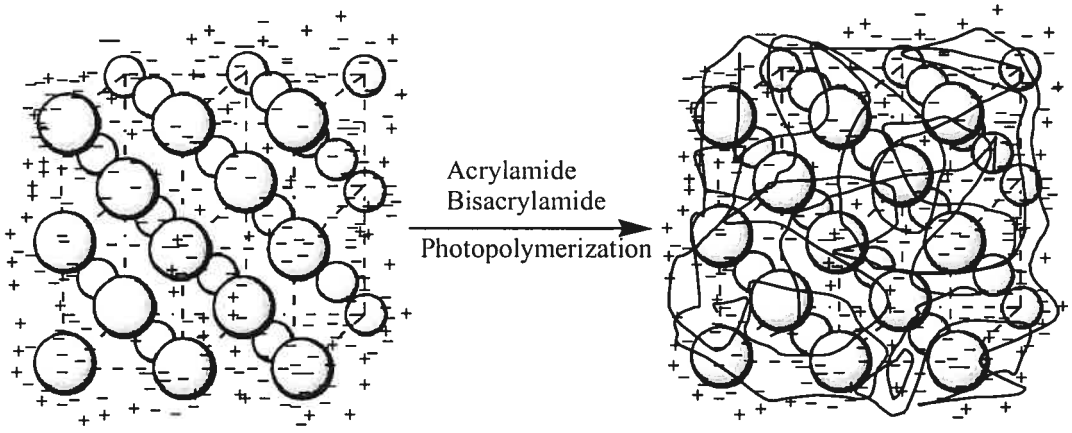

Figure 1.6. Fabrication of PCCA of charged polystyrene (copied and modified from original in ref. 53).

1.4. Biotin-avidin interaction

1.4.1. Biotin

Biotin, or hexahydro-2-oxo-1*H*-thieno[3,4-*d*]imidazole-4-pentanoic acid, is a water-soluble vitamin belonging to the B-complex, which is found in small quantities in all living cells. It exists in many isomeric forms, but only D-(+)-biotin and its derivatives are biologically active.

Biotin is synthesized in various bacteria and higher plants.[65,66] However, several microorganisms as well as higher animals are not capable of synthesizing biotin and their needs in this vitamin are met by dietary intake.[67] In nature, biotin is found either free or covalently bound to proteins or peptides.[68] The structural formulations of biotin and its main derivatives are shown in Figure 1.7.

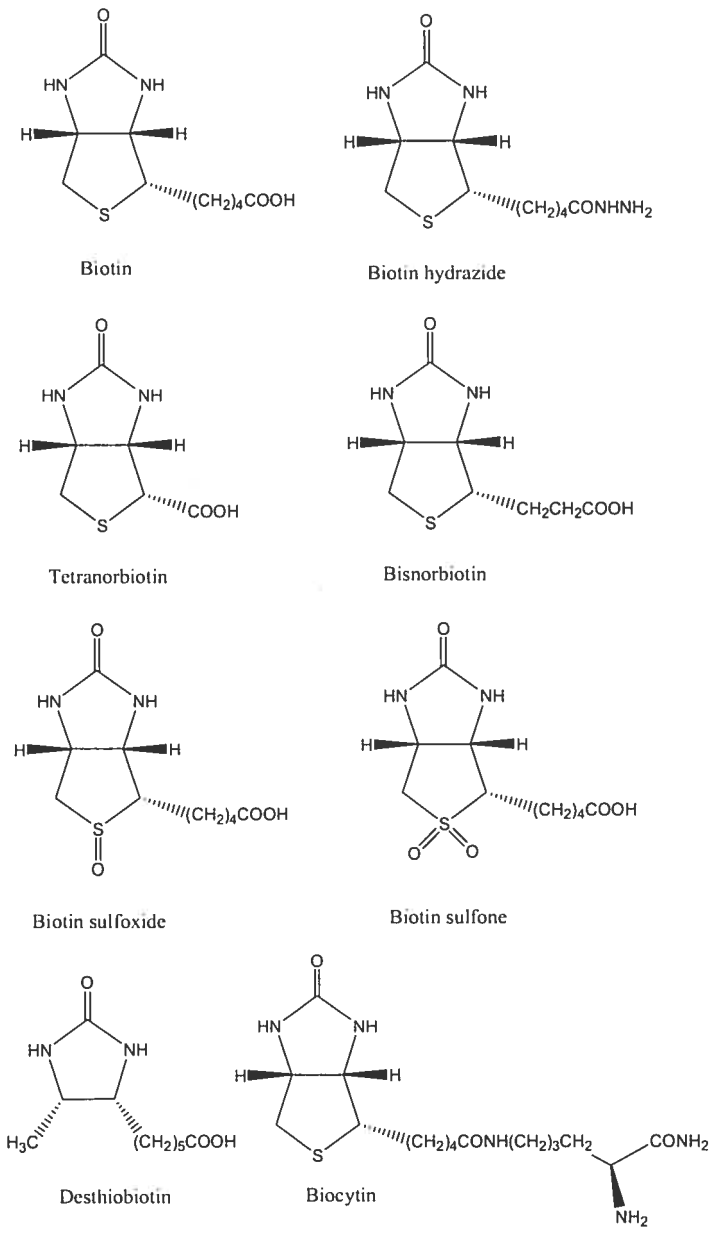

Figure 1.7. Structural formulations of biotin and its main derivatives.

The richest dietary sources of biotin include liver, kidneys, heart, pancreas, poultry, egg yolk and milk. Smaller amount is found in plants, mainly in seeds. The dietary biotin intake in human being in Western countries has been estimated to be 35 to 70 μg/day, which seems to be absorbed almost completely.[68] Biotin is involved in the biosynthesis of fatty acids, gluconeogenesis, energy production, and the metabolism of the amino acids L-leucine, L-isoleucine and L-valine.[69] Recent research results indicate

that biotin plays an important role in gene expression and that presumably it may also play a role in DNA replication.[69,70] Low biotin intake has been studied to result in severe biochemical disorders in animal organisms, such as inhibition of protein and RNA synthesis, reduced carboxylase activity and antibody production. It has indicated that biotin is involved in several animal syndromes, such as the avian fatty liver and kidney syndrome (FLKS) and the "blue slime" disease of salmonids.[67,65-71] Thus, the detection of the biotin level is very important for diagnosis.

1.4.2. Avidin and streptavidin

The early history of the protein avidin is closely related to the discovery, isolation, and synthesis of biotin. Although avidin accounts for only 0.05 % of the proteins of egg white, its presence was betrayed by an unusual dermatitis in rats fed with dried egg white as the sole source of protein.

Avidin (Figure 1.8)[72] is a basic glycoprotein with its isoelectric point at pH 10. It is very soluble in water and salt solutions, and it is stable over a wide range of pH and temperature. Avidin purified on carboxymethyl cellulose and then crystallized appears to contain two or three components when chromatographied on Amberlite CG-50 resin. It crystallizes from strong salt solution between pH 5 and 7, but it has not yet been crystallized in the isoelectric region. In contrast, streptavidin has no carbohydrate, and it has an acid isoelectric point. Therefore, it is much less soluble in water and can be crystallized from water or from 50 % isopropanol. Some basic properties of avidin and streptavidin are listed in Table 1.2.[73,74]

The gene for streptavidin has been cloned and sequenced with the ultimate objective that it can be used in general expression systems for detecting and isolating fusion proteins.[73-74] It codes for a sequence of 159 amino acids, some 30 residues longer than avidin and longer than that expected from molecular weight measurements. It was found that subunits of both low and high molecular weight are present and that the smallest one, the main constituent of most commercial preparations, is the result of the processing at both the N and C termini to give "core" streptavidin of 125-127 residues. It has a much higher solubility in water than the solubility of unprocessed precursor. This core is identical at 33 % of its residues to avidin, including the four tryptophan

residues involved in the biotin-binding site. It also resembles avidin in its predicted secondary structure, predominantly β strands and bends, and in other features (Table 1.2). Some commercial preparations contain unprocessed streptavidin, and published purification methods based on iminobiotin columns yields this as the main product.[73,74]

Table 1.2. Properties of avidin and streptavidin (copied and modified from original in refs. 73 and 74).

Property	Avidin egg white	Streptavidin	Avidin egg yolk
Amino acid residues	128	125-127	—
Subunit size (Da)			
From sequence	15,600	13,400	—
SDS gels	16,400	14,500	19,000
Subunits	4	4	4
Isoelectric pH	10	5-6	4.6
ε_{280} ($M^{-1}cm^{-1}$)	24,000	34,000	—
$\Delta\varepsilon_{233}$ (+ biotin) ($M^{-1}cm^{-1}$)	24,000	8,000	7,000
Fluorescence			
λ_{max} (nm)	338 (328)	—	—
τ (nsec)	1.8 (0.8)	—	—
K_d biotin (M) (pH 7.25)	0.6×10^{-15}	4×10^{-14}	1.7×10^{-12}
$t_{1/2}$ (days)	200	2.9	0.07

ε_{280} is absorbance coefficient at wavelength of 280 nm. $\Delta\varepsilon_{233}$ is the difference between in the presence and absence of biotin at wavelength of 233 nm. λ_{max} is the wavelength of the maxmum of fluorescence peak. τ is fluorescence lifetime. K_d is dissociation constant. $t_{1/2}$ is half life of dissociation.

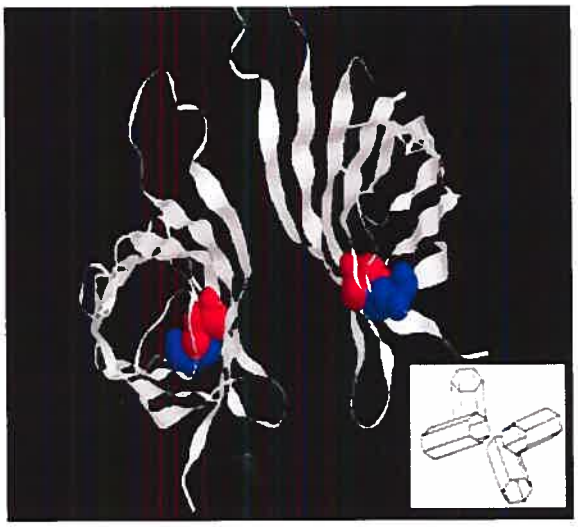

Figure 1.8. Ribbon diagram of chicken egg white avidin (see inset for tetramer configuration, copied and modified from original in ref. 77).

Two differences between streptavidin and avidin are of some importance. Streptavidin contains no carbohydrate, and it has a slightly acid isoelectric point (pH 5-6), which much minimizes non-specific absorption to nucleic acids and negatively charged cell membranes. Avidin contains carbohydrate, the heterogeneity of which is the probable cause of the poor quality of avidin crystals.

1.4.3. Biotin-avidin binding

The main common features of biotin binding by both avidin and streptavidin (Table 1.2) can be summarized briefly. Avidin and streptavidin are stable tetramers with 2-fold symmetry, which can bind up to four molecules of biotin with the binding sites being arranged in two pairs on the opposite faces of the molecule.[73-74] The stability is greatly enhanced by biotin binding, since the total free energy of binding is about 330 kJ/mol for each tetramer ($K_a = \sim 10^{15}$ M^{-1}).[73,74] The dissociation constant for biotin is so low that it can be estimated only from the ratio of the rate constants of binding and exchange using radioactive-labelled techniques. Both avidin and streptavidin are tetramers of four identical subunits which could be folded into an eight-stranded antiparallel β-barrel (Figure 1.8). Within each tetramer, biotin binding sites are located in a deep pocket in the core of the tetramer by hydrogen bonding and van der Waals

interactions. The binding sites consist of tetramer residues and a loop of the adjacent tryptophan (Trp 110) subunit. Moreover, the binding pocket is partly closed in its outer rim by a residue Trp 110 of a neighboring subunit. Once bound, biotin is almost completely buried in the protein core, with the exception of the valeryl side-chain carboxylate group which is exposed to the solvent. Two Trp residues (Trp 70 and Trp 97) are in close contact with biotin. The binding is accompanied by a red shift of the Trp spectrum and by a decrease in fluorescence; both can be used as the basis for quantitative assays.[73-75] The spectral changes in the tryptophan residues are accompanied by a remarkable reduction in their accessibility to reagents such as *N*-bromosuccinimide. In avidin, the tryptophans of each subunit are protected when biotin is bound. In contrast, fluorescence quenching by oxygen is not diminished in the avidin-biotin complex; if any, the rate constant for quenching increased.[76] The binding of biotin can be blocked or weakened by oxidation of any of some tryptophan residuse of avidin and streptavidin. For example, the binding constant is reduced to be $K_a = 10^9$ M^{-1} using periodate as oxidation agent,[77] or the binding can be weakened by the dinitrophenylation of what appears to be a single lysine residue.[77] Reaction of any one of two lysines or three tryptophans led to inactivation, and blocked or weakened further biotin binding. It is predicted that the modification on biotin can lead to weakening the binding as well.

1.4.4. Biotinylation techniques

Different biotinylation agents (Table 1.3) were used in the lsiterature.

Table 1.3. Commercially available biotinylation agents.

Biotinylation agent	The analogs
Target groups: Amine	
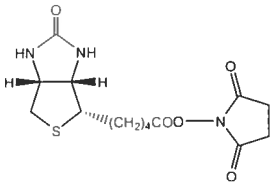 *N*-Hydroxysuccinimido biotin	Succinimidyl-6-(biotinamido) hexanoate; *N*-Hydroxysuccinmide imminobiotin. Sulfo-succinimido biotin acid Sulfo-succinimidyl-6-(biotinamido)-hexanoate; 6-Biotinamidocaproylamido)caproic acid *N*-hydroxy succinimide ester; Sulfo-succinimidyl-2-(biotinamido)ethyl-1,3-dithio propionate.
Target groups: Thiol	
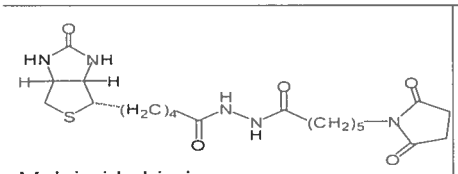 Maleimido biotin	*N*-Biotinyl-*N*-(3-maleimidopropionyl)-L-lysine; 4,4-Maleimidomethyl)cyclohexane carboxyamido) butane; Biotinyl-3-maleimidopropionamidyl-3,6-dioxaoctane diamine.
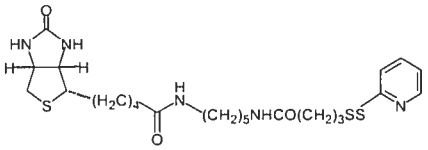 *N*-(6-(Biotinamido)hexyl)-3-(2-pyridylthio) propionate	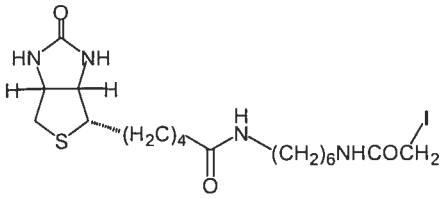 *N*-Iodoacetyl-*N*-biotinylhexylenediamine
Target groups: Aldehydes and carboxyls	
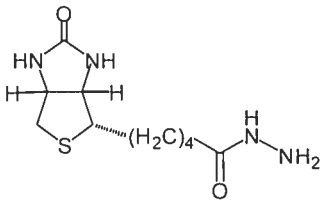 Biotinyl hydrazide	Biotin-ε-aminocaproyl hydrazide; *N*-Aminoxymethylcarbonylhydrazino biotin.
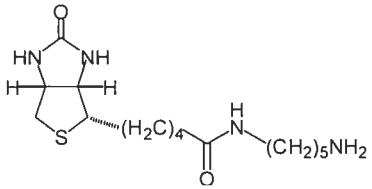 5-(Biotinamido) pentylamine	Biotin-PEO3-Amine; Biotin-PEO12-Biotin.

Biotinylation of amines. Biotinylation of amine groups was popularized with the succinimidyl esters of biotin (NHS-biotin) in DMSO or DMF (Figure 1.9). Non-sulfo agents may be preferred for soluble proteins if organic solvents are acceptable, because hydrolysis can be better controlled. They also allow intracellular labeling. NHS-biotins prefer to react with primary amine at pH 7-9, which is an ideal reagent for antibody and DNA biotinylation. The sulfosuccinimidyl ester of biotin (sulfoNHS-biotins), a more water soluble biotinylation reagent, is extensively used as topological probe to label proteins in the outer membrane surface, or when the use of organic solvents should be avoided.[78-80]

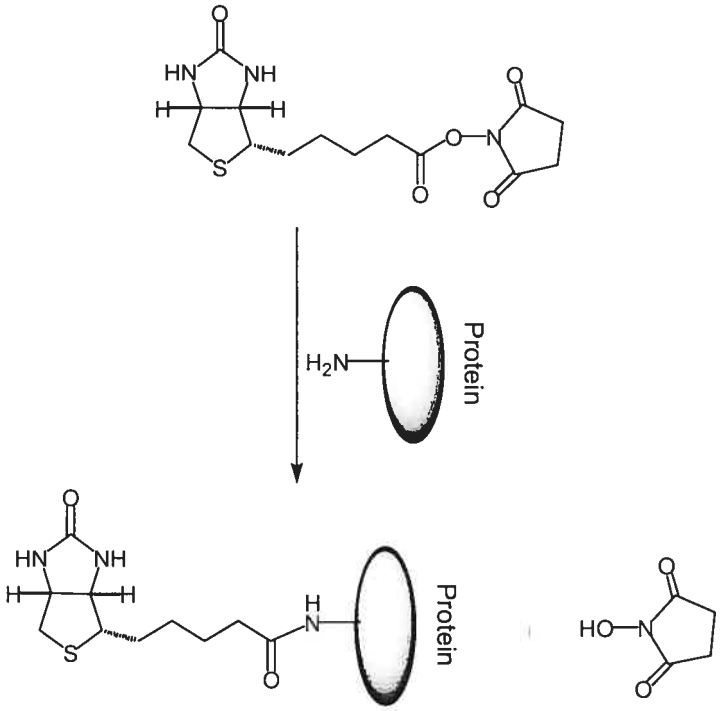

Figure 1.9. Biotinylation of amine groups of proteins.

Biotinylation of thiols. Sulfhydroxyl biotinylation is useful for the detection or modification of sites containing SH groups or the study of SH dependent structures (Figure 1.10). It also works when SH groups are introduced into proteins, peptides and nucleotides, which are thiol-modified for similar goals. In classical biotinylation

applications, the maleimido-biotin or its more soluble maleimido-lc-biocytin and maleimido-PEO3-biotin are recommended, due to their quick, quasi-stoichiometric and very specific reactivity. Maleimide reacts specifically with free sulphydryls at pH 6.5-7.5, allowing more defined labeling of proteins and avoiding undesired amine modification on proteins.[81-83]

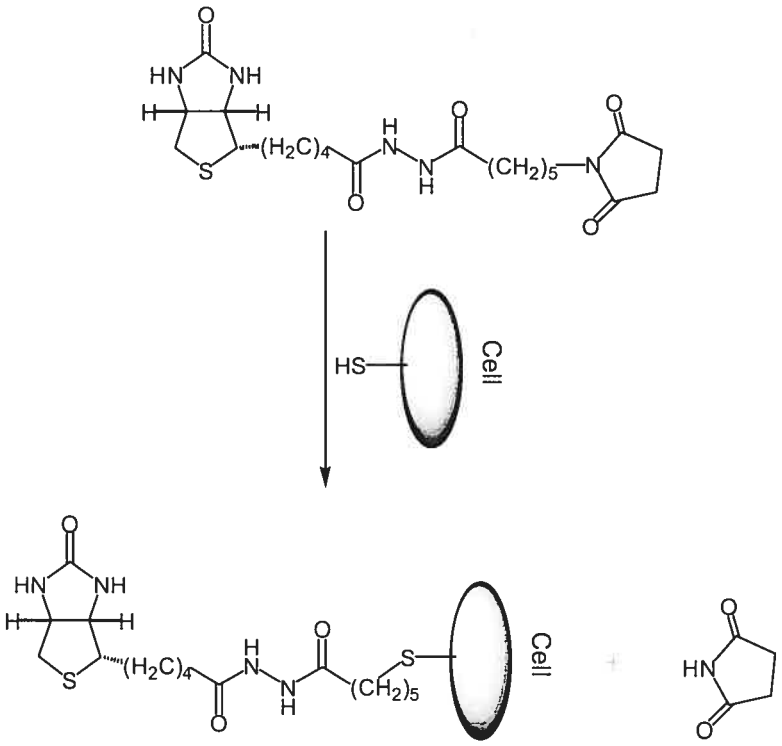

Figure 1.10. Biotinylation of thiols groups of cells.

Biotinylation of aldehydes and carboxyls. Aldehydes generated by periodate oxidation of vicinal diols, and carboxyls activated by EDAC (*N*-ethyl-*N'*-(3-dimethylaminopropyl)carbodiimide hydrochloride), can be biotinylated by using biotin hydrazides (Figure 1.11). Biotinylation could be used in glycoproteins, polysaccharides and sialic acids, steroids, glycolipids, LDL (*β*-Lipoprotein), and nucleic acids. Biotin hydrazide, a classical carbohydrate reactive biotinylation reagent, reacts with aldehydes at pH 4-6 giving a stable CH=N-NH- bound allowing the labeling of glycoproteins through their glycan. Biotin hydrazide also reacts with carboxyls in the presence of EDAC.[84-86]

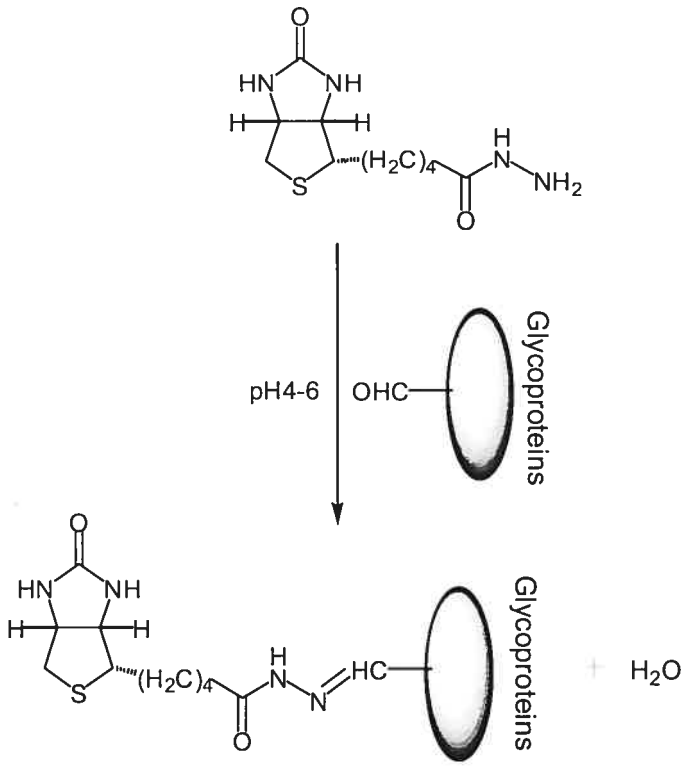

Figure 1.11. Biotinylation of aldehyde groups of glycoproteins.

1.5. Objectives

The main objective of this thesis is to design and prepare multi-responsive polymeric systems, which can be post-functionalized by bio-molecules for eventual bio-sensing applications. In this project, we have the following specific research objectives:

(1) Thermosensitive microspheres with controlled sizes will be synthesized by emulsion polymerization. The variation and control of the sizes of the microspheres will be studied.

(2) These microspheres will be used to fabricate CCAs and the packing mechanism of CCAs will be studied by microscopy and light diffraction technique. The ordered microspheres (CCA) will be immobilized in both nonthermosensitive and thermosensitive matrices to make PCCA films by photopolymerization. The thermo-optical behaviors of PCCA films will be investigated.

(3) Thermosensitive microspheres with advanced core-shell structure will be prepared by soap-free emulsion polymerization. The core-shell structure and the shrinking behaviors will be studied.

(4) To build a model sensor, biotin, a small biomolecule, is to be attached on the microspheres. Fluorescence technique will be employed to study the interaction between (strept)avidin and biotin on the microspheres. Furthermore, biotin will be attached onto a nonthermosensitive matrix of PCCA films. The interaction of avidin to the biotinylated PCCA will be studied.

The results for the first two subjects will be presented and discussed in chapter 2 and the results of the third subject will be included in chapter 3. These two chapters are presented in the form of research papers. The results for the last part will be the subject of chapter 4.

1.6. References

(1) Hoffman, A. S.; Stayton, P. S. *Macromol. Symp.* **2004**, *207*, 139-152.

(2) McCormick, C. L., editor, *Stimuli-responsive water soluble and amphiphilic polymers.* ACS symposium series, vol. 780. Washington, DC: The American Chemical Society; 2001.

(3) Laschewsky, A.; Lötsh, D.; Seeboth, A.; Storsberg, J.; Stumpe, J. Proceedings of the European coating conferences, Berlin, Germany. Vol. Smart Coating III 2004; p. 1-16.

(4) Kröger, R.; Menzel, H.; Hallensleben, M. L. *Macromol. Chem. Phys.* **1994**, *195*, 2291.

(5) Koňák, Č.; Rathi, R. C.; Kopeček, J.; *Macromolecules* **1997**, *30*, 5553.

(6) Laschewsky, A.; Rekaï, E. D. *Macromol. Rapid Commun.* **2000**, *21*, 937.

(7) Desponds, A.; Freitag, R. *Langmuir* **2003**, *19*, 6261.

(8) Ivanov, A. E.; Eremeev, N. L.; Wahlund, P. O.; Galaev, I. Y.; Mattiasson, B. *Polymer* **2000**, *43*, 3819.

(9) Akiyama, H.; Tamaoki, N. *J. Polym. Sci., Polym. Chem. A* **2004**, *A42*, 5200.

(10) Pieroni, O.; Fissi, A.; Angelini, N.; Lenci, F. *Acc. Chem. Res.* **2001**, *34*, 9.

(11) Anton, P.; Heinze, J.; Laschewsky, A. *Langmuir* **1993**, *9*, 77.

(12) Anton, P.; Laschewsky, A.; Ward, M. D. *Polym. Bull.* **1995**, *34*, 331.

(13) Mulfort, K. L.; Ryu, J.; Zhou, Q. *Polymer* **2003**, *44*, 3185.

(14) Isaksson, J.; Tengstedt, C.; Fahlman, M.; Robinson, N.; Berggren, M. *Adv. Mater.* **2004**, *16*, 316.

(15) Martin, T. J.; Prochakza, K.; Munk, P.; Webber, S. E. *Macromolecules* **1996**, *29*, 6071.

(16) Robinson, D. N.; Peppas, N. A. *Macromolecules* **2002**, *35*, 3668.

(17) Gohy, J. F.; Varshney, S. K.; Jérôme, R. *Macromolecules* **2001**, *34*, 3361.

(18) Katono, H.; Sanui, K.; Ogata, N.; Okano, T.; Sakurai, Y. *Polymer J.* **1991**, *23*, 1179.

(19) Katono, H.; Maruyama, A.; Sanui, K.; Ogata, N.; Okano, T.; Sakurai, Y. *J. Control. Release* **1991**, *16*, 215.

(20) Sasase, H.; Aoki, T.; Katono, H.; Sanui, K.; Ogata, N.; Ohta, R.; Kondo, T.; Okano, T.; Sakurai, Y. *Makromol. Chem. Rapid Commun.* **1992**, *13*, 577.

(21) Bokias, G.; Staikos, G.; Ilipoulos, I.; Audebert, R. *Macromolecules* **1994**, *27*, 427.

(22) Bekturov, E. A.; Bimendina, A. *Adv. Polym. Sci.* **1981**, *41*, 99.

(23) Staikos, G.; Bokias, G.; Karayanni, K. *Polymer Inter.* **1996**, *41*, 345.

(24) Ito, S.; Hirasa, O.; Yamauchi, A. *Kobunshi Ronbunshu* **1989**, *46*, 427.

(25) Platé, N. L.; Lebedeva, T. L.; Valuev, L. I. *Polymer J.* **1999**, *31*, 21.

(26) Schild, H. G. *Prog. Polym. Sci.* **1992**, *17*, 163.

(27) Hoffman, A. *Controlled Drug Delivery. Challenges and Strategies*. Park, K., Ed.: American Chemical Society: Washington, DC, 1997; pp 485-498.

(28) Park, T. G. *Biomaterials* **1999**, *20*, 517.

(29) Ichikawa, H.; Fukumori, Y. *J. Control. Release* **2000**, *63*, 107.

(30) Kim, S. W.; Bae, Y. H.; Okano, T. *Pharm. Res.* **1992**, *9*, 283.

(31) Miyata, T.; Asami, N.; Uragami, T. *Macromolecules* **1999**, *32*, 2082.

(32) Waler, J. P.; Asher, S. A. *Anal. Chem.* **2005**, *77*, 1596.

(33) Kawaguchi, H.; Fujimoto, K. *Bioseparation* **1998**, *7*, 253.

(34) Kayaman, N.; Kazan, D.; Erarslan, A.; Okay, O.; Baysal, B. M. *J. Appl. Polym. Sci.* **1998**, *67*, 805.

(35) Umeno, D.; Kawasaki, M.; Maeda, M. *Bioconjugate Chem.* **1998**, *9*, 719.

(36) Chen, L.; Kopecek, J.; Stewart, R. J. *Bioconjugate Chem.* **2000**, *11*, 734.

(37) Stile, R. A.; Burghardt, W. R.; Healy, K. E. *Macromolecules* **1999**, *32*, 7370.

(38) Stile, R. A.; Healy, K. E. *Biomacromolecules* **2001**, *2*, 185.

(39) Bergbreiter, D. E.; Case, B. L.; Liu, Y. S.; Caraway, J. W. *Macromolecules* **1998**, *31*, 6053.

(40) Bergbreiter, D. E.; Liu, Y. S.; Osburn, P. L. *J. Am. Chem. Soc.* **1998**, *120*, 4250.

(41) Nagayama, H.; Maeda, Y.; Shimasaki, C.; Kitano, H. *Macromol. Chem. Phys.* **1995**, *196*, 611.

(42) Hiltner, P. A.; Krieger, I. M. *J. Phys. Chem.* **1969**, *73*, 2386.

(43) Dinsmore, A. D.; Crocher, J. C.; Yodh, A. G. *Curr. Opin. Colloid Interface Sci.* **1998**, *3*, 5.

(44) Pusey, P. N.; van Megen, W. *Nature* **1986**, *320*, 340.

(45) Cheng, Z. D.; Zhu, J. X.; Russel, W. B.; Chaikin, P. M. *Phys. Rev. Lett.* **2000**, *85*, 1460.

(46) Velev, O. D.; Kaler, E. W. *Adv. Mater.* **2000**, *12*, 531.

(47) Jiang, P.; Hwang, K. S.; Mittleman, D. M.; Bertone, J. F.; Colvin, V. L. *J. Am. Chem. Soc.* **1999**, *121*, 11630.

(48) Yablonovitch, E.; Gmitter, T. J. *Phys. Rev. Lett.* **1989**, *63*, 1950.

(49) Lee, W.; Pruzinsky, S. A.; Braun, P. V. *Adv. Mater.* **2002**, *14*, 271.

(50) Vlasov, Y. A.; Deutsch, M.; Norris, D. J. *Appl. Phys. Lett.* **2000**, *76*, 1627.

(51) Reese, C. E.; Mikhonin, A. V.; Kamenjicki, M.; Tikhonov, A.; Asher, S. A. *J. Am. Chem. Soc.* **2004**, *126*, 1493.

(52) Weissman, J. M.; Sunkara, H. B.; Tse, A. S.; Asher, S. A. *Science* **1996**, *274*, 959.

(53) Asher, S. A.; Alexeev, S. A.; Goponenko, A. V.; Sharma, A. C.; Lednev, I. K.; Wilcox, C. S.; Finegold, D. N. *J. Am. Chem. Soc.* **2003**, *125*, 3322.

(54) Hellweg, T.; Dewhurst, C. D.; Brückner, E.; Kratz, K.; Eimer, W. *Colloid Polym. Sci.* **2000**, *278*, 972.

(55) Debord, J. D.; Eustis, S.; Debord, S. B.; Lofye, M. T.; Lyon, L. A. *Adv. Mater.* **2002**, *14*, 658.

(56) Debord, S. B.; Lyon, L. A. *J. Phys. Chem. B* **2003**, *107*, 2927.

(57) Lyon, L. A.; Debord, J. D.; Eustis, S.; Debord, S. B.; Jones, C. D.; McGrath, J. G.; Serpe, M. J. *J. Phys. Chem. B* **2004**, *108*, 19099.

(58) Spry, R. J.; Kosan, D. J. *Appl. Spectrosc.* **1986**, *40*, 782.

(59) Chutinan, A.; Noda, S. *Phys. Rev. B: Condens. Mater.* **2000**, *62*, 4488.

(60) Ye, Y. H.; LeBlanc, F.; Hache, A.; Truong, V. V. *Appl. Phys. Lett.*, **2001**, *78*, 52.

(61) Ye, Y. H.; Mayer, T. S.; Khoo, L. C.; Divliansky, I. B.; Abrams, N.; Mallouk, T. E. *J. Mater. Chem.*, **2002**, *12*, 3637.

(62) Holtz, J. H.; Asher, S. A. *Nature* **1997**, *389*, 829.

(63) Nayak, S.; Debord, J. D.; Lyon, L. A. *Langmuir* **2003**, *19*, 7374.

(64) Hu, Z.; Lu, X.; Gao, J. *Adv. Mater.* **2001**, *13*, 1708.

(65) Baldet, P.; Alban, C.; Douce, R. *Methods Enzymol.* **1997**, *279*, 327.

(66) Katakeyama, K.; Kobayashi, M.; Ykawa, H. *Methods Enzymol.* **1997**, *279*, 339.

(67) Bonjour, J. P. in: Machlin, L. J. (Ed), *Handbook of Vitamins*, Marcel Dekker, New York, 1984, p 403.

(68) Zempleni, J.; Mock, D. M. *J. Nutr. Biochem.* **1999**, *10*, 128.

(69) Vilches-Flores, A.; Fernandez-Mejia, C. *Rev. Invest. Clin.* **2005**, *57*, 716.

(70) (a) Whitehead, C. C. *Ann. N. Y. Acad. Aci.* **1985**, *447*, 86; (b) Bonjour, J. P. *Ann. N. Y. Acad. Aci.* **1985**, *447*, 97.

(71) Watkins, B. A. *Br. J. Nutr.* **1988**, *61*, 99.

(72) http://www.chemistry.unimelb.edu.au/staff/mlgee/research/PSI/mclean.html

(73) Green, N. M. *Methods Enzymol.* **1990**, *184*, 51.

(74) Green, N. M. *Methods Enzymol.* **1970**, *18*, 418.

(75) Lin, H. J.; Kirsch, J. F. *Methods Enzymol.* **1990**, *62*, 287.

(76) Maliwal, B. P.; Lakowicz, J. *Biophys. Chem.* **1985**, *19*, 337.

(77) Green, N. M. *Adv. Protein Chem.* **1975**, *29*, 85.

(78) Miller, B. T.; Collins, T. J.; Rogers, M. E.; Kurosky, A. *Peptides* **1997**, *18*, 1585.

(79) Veenman, C. L.; Reiner, A.; Honig, M. G. *J. Neurosci. Meth.* **1992**, *41*, 239.

(80) Petrie, C. R.; Adams, A. D.; Stamm, M.; Van Ness, J.; Watanabe, S. M.; Meyer, R. B. *Bioconjugate Chem.* **1991**, *2*, 441.

(81) Sutoh, K.; Yamamoto, K.; Wakabayashi, T. *J. Mol. Biol.* **1984**, *178*, 323.

(82) Bayer, E. A.; Zalis, M. G.; Wilchek, M. *Anal. Biochem.* **1985**, *149*, 529.

(83) Bernier, M.; Nadiv, O.; Kole, H. K. *Biochemistry* **1995**, *34*, 8357.

(84) Musso, G. F.; Scarlato, G. R.; Ghosh, S. S. *Bioconjugate Chem.* **1992**, *3*, 88.

(85) Allart, B.; Lehtolainen, P.; Yla-Herttuala, S.; Martin, J. F.; Selwood, D. L. *Bioconjugate Chem.* **2003**, *14*, 187.

(86) Blanchard, C. Z.; Chapman-Smith, A.; Wallace, J. C.; Waldrop, G. L. *J. Biol. Chem.* **1999**, *274*, 31767.

2. Preparation and Thermo-Responsive Light Diffraction Behaviors of Soft Polymerized Crystalline Colloidal Arrays*

2.1. Abstract

We report the formation and light diffraction behavior of polymerized crystalline colloidal arrays (PCCA) based on lightly cross-linked thermosensitive particles of poly(*N*,*N*-diethylacrylamide-*co*-*N*-ethylacrylamide-*co*-2-hydroxyethyl methacrylate) in both thermosensitive and non-thermosensitive matrices. The formation process of the crystalline colloidal arrays (CCA) and the temperature-dependent light diffraction behavior of PCCAs are investigated and rationalized by the use of Flory's polymer solution and rubber elasticity theories. The light diffraction behaviors of the PCCAs studied are found to display one and two temperature transitions in non-thermosensitive and thermosensitive matrices, respectively. The effects of ionic strength and pH on PCCA films have also been investigated.

2.2. Introduction

Spatial periodicity in the dielectric function of an optical material can yield both allowed and forbidden directions in which electromagnetic waves of certain energies may propagate. These photonic bandgap effects arise from coherent interferences by multiple scattering when the wavelength of the electromagnetic waves are comparable with the periodicity length of the lattice similar to X-ray diffraction by atomic crystals.[1] Such effects have been applied to design chemical and biological sensors,[2] optical waveguides,[3] optical switches,[4] and optical filters.[5] It is well-known that the self-assembly of monodispersed charged particles such as polystyrene (PS),[2,4,6] poly(*N*-isopropylacrylamide) (PNIPAM),[7] and poly(methyl

---

* Paper accepted by *Soft Matter*, November 2006. Authors: Yilong Chen, Julien E. Gautrot, Zhanyong Li, and X. X. Zhu, *Soft Matter*, 2007, *2*, 1-10.

mathacrylate)[8] produces three-dimensionally periodic structures. This phenomenon is primarily due to the electrostatic interactions of charges on the particle surface, coupled to the diffuse counterion cloud.

It was found that lightly cross-linked thermosensitive particles with lower critical swelling temperatures (LCST) could spontaneously form a crystalline colloidal array (CCA) via a simple temperature-cycling process.[9-14] The formation mechanism of such soft thermosensitive particles still remains unclear. Lyon and co-workers have demonstrated that a lightly cross-linked PNIPAM could form CAAs after concentration by centrifugation.[9-11] Their results showed that, as the effective volume fraction of the microgel colloidal crystals (ϕ_{eff}) decreased (by reducing the polymer concentration), the lattice constant increased and the crystal eventually "melted" into a fluid phase at $\phi_{eff} = 0.49$. Similarly, when the temperature was raised above the LCST of the particles, their effective volume fraction decreased resulting in the "melting" of the CCA. Lyon and co-workers suggested that such phenomena could be rationalized by the introduction of compression forces between particles, acting on the equilibrium state of the CCA. However, such "soft" CCA lattices are relatively unstable and cannot directly be used in the fabrication of devices such as sensors. Asher and co-workers used polymerized CCAs (PCCAs) based on poly(styrene-*co*-styrene sulfonate) CCAs embedded in PNIPAM and polyacrylamide (PAAm) matrices.[2,4,6,7] The main advantage of PCCAs is that they possess much better thermal, chemical and mechanical stability than CCAs (Figure 2.1). However, the control of the ordered structure of CCA during matrix formation remains an issue, especially in the case of soft CCAs. Lyon and co-workers reported that the order was lost upon photopolymerization of a NIPAM matrix embedding PNIPAM CCAs.[12]

If a simple method for the preparation of PCCAs with soft particles in a soft matrix can be developed, such hydrophilic composite materials may reveal very promising properties for biosensing applications. A good fundamental understanding of such systems is key to their potential applications. To the best of our knowledge, there have been only a very limited number of reports on this subject. Asher and co-workers reported that PCCAs constituted of charged PNIPAM in PAAm can be used

as optical switch, triggered by temperature changes, on the nanosecond scale.[4] The diffractive intensity of these PCCAs was increased by heating, while the diffracted wavelength remained unchanged. Hu and co-workers successfully cross-linked PNIPAM particles with epichlorohydrin and divinylsulfone (DVS) to produce "hydrogel opals", which responded to changes in temperature and solvents.[13] Lyon and co-workers studied the deswelling behavior of microcomposite hydrogel films composed of lightly cross-linked PNIPAM particles in PNIPAM matrix,[12] where the ordered structure of the particles was not preserved upon photopolymerization.

Here, we report here the preparation of CCA of lightly crosslinked thermosensitive particles *via* a simple temperature-cycling process. We chose to use polyacrylamides in conjunction with HEMA to provide free hydroxyl groups that can be post-functionalized. The temperature and concentration effects were investigated to gain further understanding of the formation mechanism of CCAs. PCCAs of uncharged thermosensitive CCAs in both non-thermosensitive and thermosensitive polymer matrices have been prepared. The shrinkage upon photopolymerization of the matrix and its dependence on the concentration of particles forming the CCA have been studied. The effect of temperature on the PCCAs of thermosensitive particles in non-thermosensitive matrices has been investigated and rationalized by the use of Flory's polymer solution and rubber elasticity theories.[15-17] In the case of PCCAs with thermosensitive matrices, two volume phase transitions (VPT), corresponding to the matrix and the particles forming the CCA, respectively, were found to affect the light diffraction phenomenon. Finally, the effects of pH and ionic strength on the different PCCA films formed were investigated.

2.3. Experimental section

2.3.1. Materials

All chemicals were purchased from Aldrich and used without further purification unless otherwise stated. Distilled water was purified by a Millipore water purification system. 2-hydroxyethyl methacrylate (HEMA) was distilled under

reduced pressure prior to use. NIPAM was recrystallized in acetone. *N*,*N*-diethylacrylamide (DEA) and *N*-ethylacrylamide (EA) were prepared according to the literature.[18] *N*,*N'*-methylenebisacrylamide (BA) was recrystallized from methanol.

2.3.2. Synthesis of thermosensitive microspheres

In a typical procedure, the thermosensitive microspheres were prepared by emulsion polymerization in a tri-neck flask equipped with a mechanical stirrer (625 rpm). The monomers (33.3 mmol DEA, 22.2 mmol EA, and 23.7 mmol HEMA), BA (1.2 mmol) and sodium dodecylsulfate (SDS, 2.2 mmol) were added to 1000 ml of stirred milli-Q water followed by nitrogen purging for 30 minutes at 70 °C. Polymerization was initiated by the addition of a solution of potassium persulfate (KPS, 1.8 mmol in 15 ml of Milli-Q water) to the vigorously stirred mixture. The reaction was stopped after 4 h and allowed to cool down to room temperature. Filtration of the milky suspension through a 2.0 μm Millipore Isopore^{TM} membrane filter (Sigma), followed by centrifugation and dialysis for 14 days in a cellulose sack (Sigma, MW > 12,000) afforded pure microparticle solutions at a concentration of 31.1 wt%.

2.3.3. Preparation of PCCAs

CCAs were prepared via a simple temperature cycling between 10 and 45 °C of a solution containing the thermosensitive microspheres (LCST around 20 °C) at the desired concentration. In a typical procedure, 2 g of a CCA latex at the desired concentration, 100 mg of the monomer (AAm, *N*,*N*-dimethylacrylamide (DMA), DEA, or NIPAM), 10 mg BA (cross-linker), and 50 μl diethoxyacetophenone (DEAP, 10 vol% in DMSO) were placed in a chamber gasket (0.5 mm thickness, Molecular Probe) covered with a quartz slide at 5 °C, and subsequently irradiated under UV light (365 nm) for 10 h. The resulting films were soaked in Milli-Q water for 7 days (medium changed daily) to remove chemical residues, and as to swell the PCCAs to their equilibrium state (Figure 2.1).

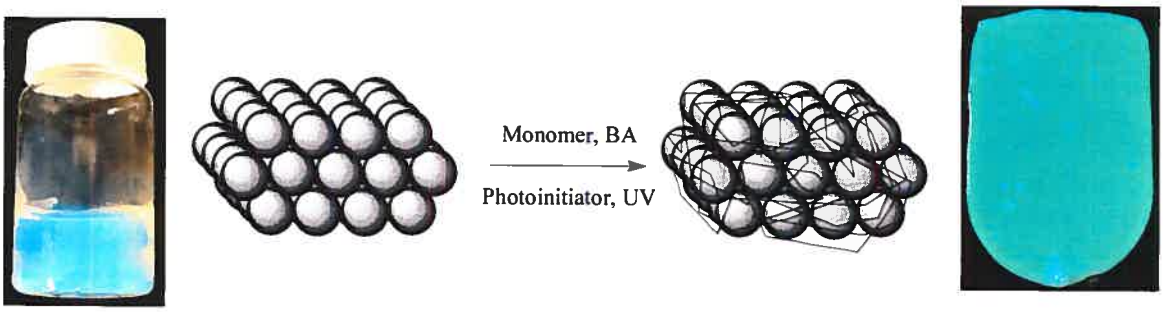

Figure. 2.1 Preparation of PCCAs (hypothetical packing structure).

2.3.4. Dynamic light scattering

Dynamic light scattering (DLS) measurements were performed on a Brookhaven BI-200SM light scattering instrument set up with a Science / Electronics temperature controller and a 532 nm green JDS laser. Samples were prepared by suspending 0.1 ml of CCA latex in 20 ml of Milli-Q water, followed by filtration through a 2-μm filter. To ensure data reproducibility, measurements were taken 25 minutes after the sample temperature was stabilized. At each temperature, eight measurements were taken to determine the average diameter of the spheres, and each temperature cycle was repeated at least 3 times per sample. The standard deviation was estimated to be about 5 % as confirmed by multiple measurements obtained using the same sample after several heating and cooling cycles. In a DLS experiment the scattering light intensity autocorrelation function $g_I(t)$ is measured, which is related to the field autocorrelation function $g_1(t) = 1 + g_E^{\,2}(t)$. In the case of purely translational motion, $g_E(t) = e^{-t/\tau}$ and $\frac{1}{\tau} = q^2 D$, where τ is the relaxation time and D the diffusion coefficient, were used. From D, a hydrodynamic diameter R_h is calculated using Stokes-Einstein relation $D = kT / (3\pi\eta R_h)$, which holds for non-interacting spheres. T denotes the temperature and η the viscosity of the solvent. In the case where a relaxation time distribution $G(\ln \tau)$ must be used, $g_E(t) = \int_{\ln \tau_{min}}^{\ln \tau_{max}} G(\ln \tau) e^{-t/\tau} d \ln \tau$, which is obtained from $g_E(t)$ by Quadratic analysis.

2.3.5. Visible light diffraction

CCAs and PCCAs diffract light in accordance with the Bragg's law

$$m\lambda = 2nd\sin\theta \quad (1)$$

where m is the order of diffraction, λ the wavelength of incident light, n the refractive index of the suspension, d the interplanar spacing, and θ the glancing angle between the incident light and the diffracting crystal planes, oriented parallel to the crystal surface. Diffraction measurements were taken on a home-assembled spectrophotometer (Gamble Technologies USB2000) with wavelength coverage between 350-1000 nm and equipped with a tungsten halogen light source and a R200-7 VIS/NIR reflection probe (Ocean Optics). Diffraction spectra were normalized to allow easy comparison. The prepared PCCA films were fragmented to obtain homogeneous samples and the spectra were recorded in a UV cuvette. The temperature was controlled using a circulating water bath. Temperature of the sample was measured by means of a thermocouple immersed in the solution (± 0.1 °C).

2.4. Results and discussion

2.4.1. Synthesis and characterization of CCAs

Lightly cross-linked copolymers of DEA, EA and HEMA have been synthesized by emulsion polymerization (Table 2.1). EA was used to raise the LCST while the use of HEMA allows the introduction of a hydroxyl group that could be further functionalized for sensing applications. The particle size was controlled by varying the concentrations of SDS and monomers (Table 2.1).

Table 2.1 Emulsion polymerization conditions for the preparation of microgel particles.

Sample	SDS (g/L)	Total monomers (mmol/L)[a]	KPS (g/L)	$^{b}R_{h,10^{o}C}$ (nm)	Polydispersity index[b]	$^{b}R_{h,10^{o}C}/R_{h,50^{o}C}$
CCA1	0.60	79.2	0.48	387	0.08	2.28
CCA2	0.60	105.6	0.48	427	0.06	2.37
CCA3	0.24	105.6	0.36	717	0.09	2.65

[a]Feed composition of HEMA : DEA : EA = 0.3 : 0.42 : 0.28 (molar ratios) cross-linked with 1.5 mol% of BA;

[b]$R_{h,10\ ^{o}C}$ (hydrodynamic diameter at 10 °C), polydispersity index and $R_{h,10^{o}C}/R_{h,50^{o}C}$ of the particles measured by DLS.

Figure 2.2 shows the change of the hydrodynamic diameter of the particles as a function of temperature. Light diffraction behaviors of particles of various sizes were studied as a function of temperature and particle concentration. A dilute solution of microgel particles was first concentrated via centrifugation followed by dilution of the sample to the desired concentration. As shown in Figure 2.2, the particle volume typically changes by a factor larger than 8 upon increasing temperature above its LCST. In order to generate the CCAs, the temperature of the latex samples was cycled between 10 and 45 °C and diffraction spectra were taken before and after this process and recorded at 10 °C (Figure 2.3A). Before temperature cycling, the spectrum is broad and featureless, whereas after this process the thermosensitive particles spontaneously "crystallize" into a brightly iridescent material displaying a narrow and symmetrical diffraction peak with half width of 150 nm, a phenomenon also observed by Lyon and co-workers for PNIPAM CCAs.[9-12] Since the "crystallization" of the microspheres depends on their size and concentration, the large volume phase transition observed by DLS confers sufficient freedom to the particle to rearrange and adopt a thermodynamically favored configuration upon cooling below their LCST, thus forming better defined CCAs possessing sharper light diffraction features.

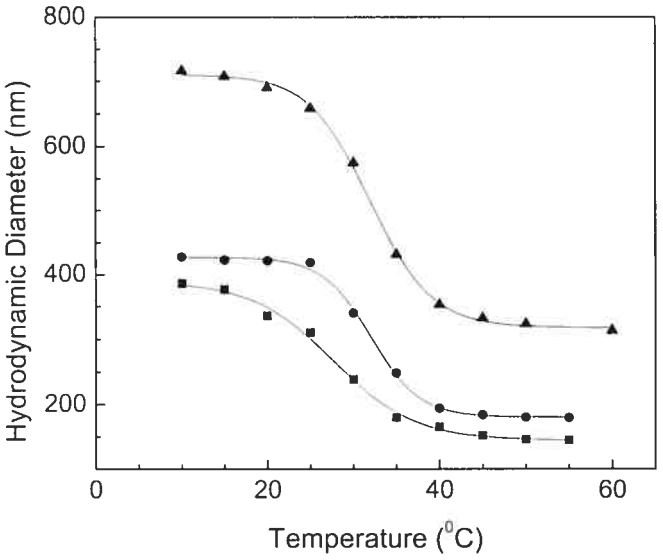

Figure 2.2 Hydrodynamic diameters of colloidal particles making CCAs **1** (■), **2** (●), and **3** (▲) as a function of temperature (measured by DLS).

The light diffraction spectra of a 7 wt% solution of **CCA1** were taken at different temperatures (Figure 2.3B). The diffraction peak increases slightly while raising temperature from 5 to 10 °C, presumably due to the increase of the refractive index of the particles with the temperature, before decreasing again above 15 °C. At 40 °C, the diffraction peak disappears completely. In the CCAs, the particles are believed to be closely packed and compressed. The particle size decreases with increasing temperature, with no change in the interparticle distance (*d*). When their hydrodynamic diameter measured by DLS becomes smaller than *d*, the particles can move freely and the CCA is disrupted. The diffraction disappears above LCST, in contrast to the observation by Asher and co-workers for the CCA of a charged copolymer, poly(NIPAM-*co*-2-acrylamido-2-methyl-1-propanesulfonic acid), showing a diffraction peak even above the LCST of this material.[6] Indeed, in their case, the assembly of the charged particles was stabilized by electrostatic repulsions and therefore did not require annealing. The formation of CCAs made of uncharged thermosensitive particles is a reversible process, which needs temperature cycling to be performed to improve the ordering of the soft particles.

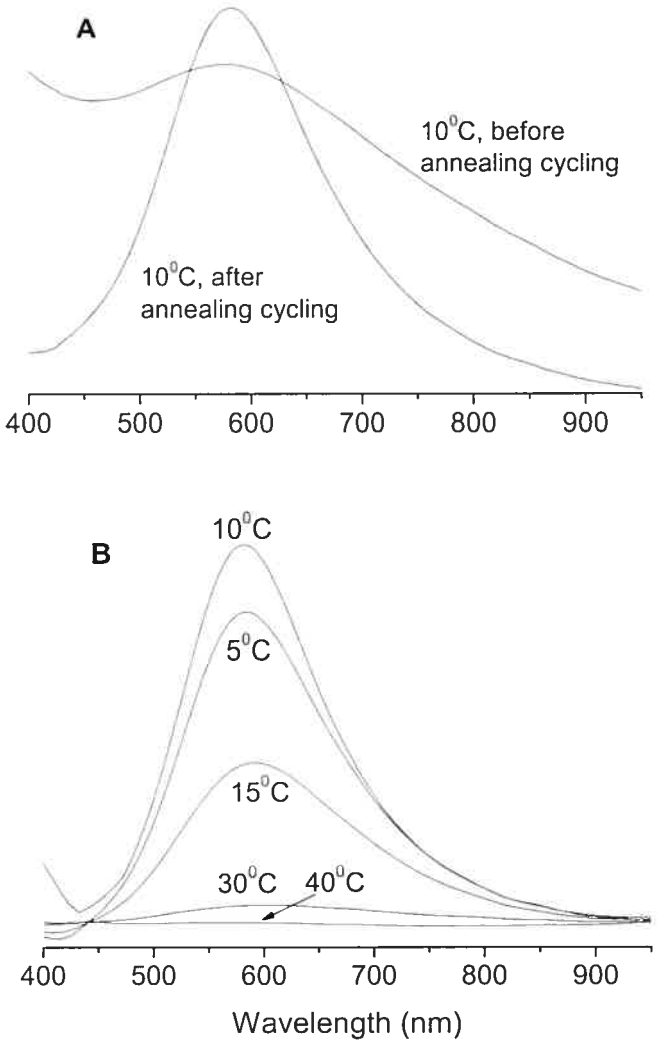

Figure 2.3 (A) Light diffraction spectra of **CCA1** (7 wt%) at 10°C before and after temperature cycling; (B) light diffraction spectra of **CCA1** (7 wt%) at different temperatures after temperature cycling.

In order to understand the CCA formation from soft microspheres, diffraction spectra were obtained at different concentrations for **CCA1** at 10 °C (Figure 2.4A). The diffraction peak undergoes a blue shift with increasing concentrations. The increased compression between the particles at higher concentrations reduces *d* and

therefore blue-shifts the diffraction peak. Such an increased compression helps in the formation of a more ordered packing structure, which may explain the obvious narrowing in the diffraction spectrum as the concentration increases. The diffraction wavelengths (λ), taken as the mass center of the spectra, are plotted as a function of particle concentration in Figure 2.4B for CCAs **1**, **2**, and **3**.

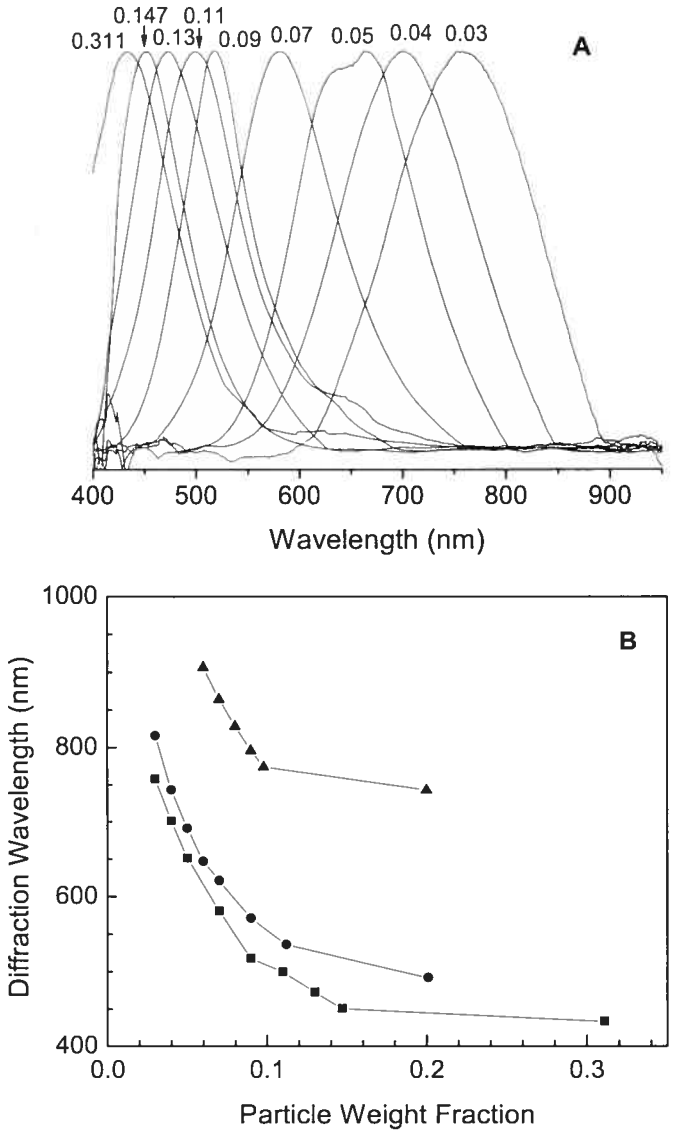

Figure 2.4 (A) Light diffraction spectra of **CCA1** at different weight fractions in water; (B) diffraction wavelength of CCAs **1** (■), **2** (●), and **3** (▲) as a function of weight fraction of the particles.

It is apparent that CCAs formed by larger particles show diffraction peaks at higher wavelengths. Therefore, it is possible to obtain photonic materials with diffraction wavelengths ranging from infrared to ultraviolet by simply adjusting the size and concentration of the particles. The interparticle distance calculated by using Bragg's law (n = 1.333) and assuming a FCC crystalline structure (as was obtained for PNIPAM)[19] is smaller than the hydrodynamic diameter of the particles at 10 °C and further decreases with increasing concentrations. The interparticle distance reaches a plateau at a certain concentration (~ 10 wt%), indicating the compression limit of the CCA, where the interparticle distance is comparable to the hydrodynamic diameter measured above LCST. At very low concentrations (< 3 wt%), the particles are too far apart, and do not form CCAs. When particle concentration is between ca. 3 and 10 wt%, the particles are compressed and form CCAs, below their LCST.

2.4.2.Preparation of PCCAs

It is well-known that PCCAs constituted of charged PS in PAAm hydrogel matrices do not display temperature sensitivity although they can be used as biological and chemical sensors.[2,4,6,7,20,21] PCCAs formed by charged PS in PNIPAM, however, display a blue shift of their diffraction wavelength with increasing temperatures.[21] Asher and co-workers reported that PCCAs constituted of charged PNIPAM in PAAm can be used as fast optical switches triggered by temperature changes.[4] PCCAs of uncharged thermosensitive particles in non-thermosensitive and thermosensitive matrices like PAAm and PNIPAM have been less studied, most probably due to their difficulty of their preparation and the complexity of their properties, but were found to display interesting properties for applications as biocompatible sensors.[12,13] Lyon and co-workers reported the deswelling behavior of PNIPAM microgel composite films upon heating and a loss of the ordered CCA structure during photopolymerization.[12] We found that it is critical to keep the reaction temperature below the LCST of the material to maintain the order during the preparation of the PCCA with soft thermosensitive microspheres. Moreover, the swollen state of the CCA below LCST allows the diffusion

of the monomers within its bulk, forming an interpenetrated polymer system upon photopolymerization.

AAm, DMA, DEA and NIPAM, which are all water-soluble, were used separately as the monomers and BA as the cross-linker to embed **CCA1**. The light diffraction spectra of CCA/monomer solutions (λ_{CCA}), PCCAs after photopolymerization (λ_{PCCA}), and PCCAs after washing and swelling in milli-Q water (λ_{20}) were measured at 20 °C (Figure 2.5). Data obtained for the different samples are gathered in Table 2.2. λ_{PCCA} was found to be smaller than λ_{CCA} due to polymerization shrinkage. After washing and swelling in water, the diffraction wavelength (λ_{20}) increases, relative to both λ_{CCA} and λ_{PCCA}. It is possible to calculate the shrinkage of the matrix by using the following equation:[2,4,6,20,21]

$$\text{Shrinkage} = (V_0 - V)/V_0 = 1 - (\lambda_{PCCA}^3 / \lambda_{CCA}^3) \quad (2)$$

where V_0 and V are the volumes before and after polymerization, respectively. From these results (Table 2.2), it is apparent that both the concentration of the starting CCA and the nature of the matrix have an important effect on the shrinkage of the film. In other composite materials, increasing amounts of fillers have also been shown to reduce polymerization shrinkage.[22,23]

Table 2.2 Optical properties of PCCAs in non-thermosensitive and thermosensitive matrices prepared at different **CCA1** concentrations.

Sample	Matrix	C_{CCA} (wt%)	λ_{PCCA} (nm)	λ_{CCA} (nm)	λ_{20} (nm)	$\Delta\lambda$ (nm)[a]	Shrinkage
PCCA1	PAAm	5	480	658	711	50.2	0.61
PCCA2	PAAm	10	466	599	685	85.3	0.53
PCCA3	PAAm	18.9	430	508	592	105.0	0.39
PCCA4	PDMA	18.9	447	509	578	106.6	0.32
PCCA5	PNIPAM	5	441	670	691	243.6	0.71
PCCA6	PNIPAM	10	417	598	642	216.9	0.66
PCCA7	PNIPAM	18.9	486	508	575	218.8	0.12
PCCA8	PDEA	18.9	485	508	572	190.6	0.13

[a]Difference between diffraction wavelengths at the starting and final temperatures.

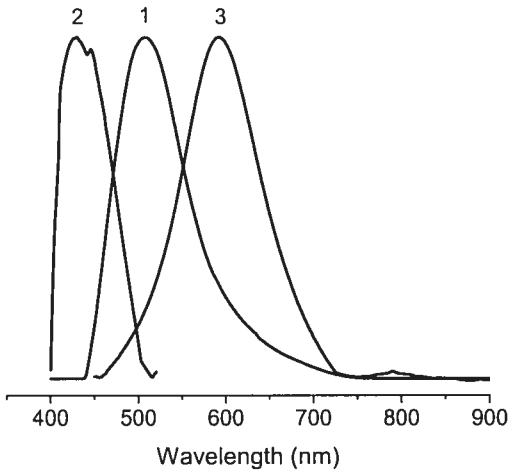

Figure 2.5 Typical diffraction spectra of **CCA1** (1), **PCCA3** just after photopolymerization (2), and **PCCA3** washed and equilibrated in water (3) at 20 °C.

2.4.3. PCCAs with non-thermosensitive matrices

The CCAs used in this study show thermo-optical properties related to the LCST of the soft particles. PCCAs in both thermosensitive and non-thermosensitive matrices also show thermo-optical properties. The case of CCAs embedded in non-thermosensitive matrices will first be discussed to distinguish the contributions of the CCA and the matrix from the opalescent phenomena.

Figure 2.6A shows the diffraction spectra of **PCCA3** at different temperatures. The peaks are narrow and symmetrical with half width of 110 nm, suggesting a well-ordered particle packing, and a well-defined periodic length. It is apparent that the diffraction spectra are blue-shifted with increasing temperature. The mass centers of the diffraction spectra versus temperature for PCCAs **1**, **2** and **3** are plotted in Figure 2.6B. The position of the inflexion correlates well with the VPT temperature or LCST of the particles, suggesting that the shrinkage of the particles in the CCA can drag the matrix along, reduce the interplanar distance, and blue-shift the diffraction spectrum. The shrinkage is apparent to the naked eye. Such an efficient dragging phenomenon is the

direct result of the interpenetration and entanglement of the particles and matrix network.

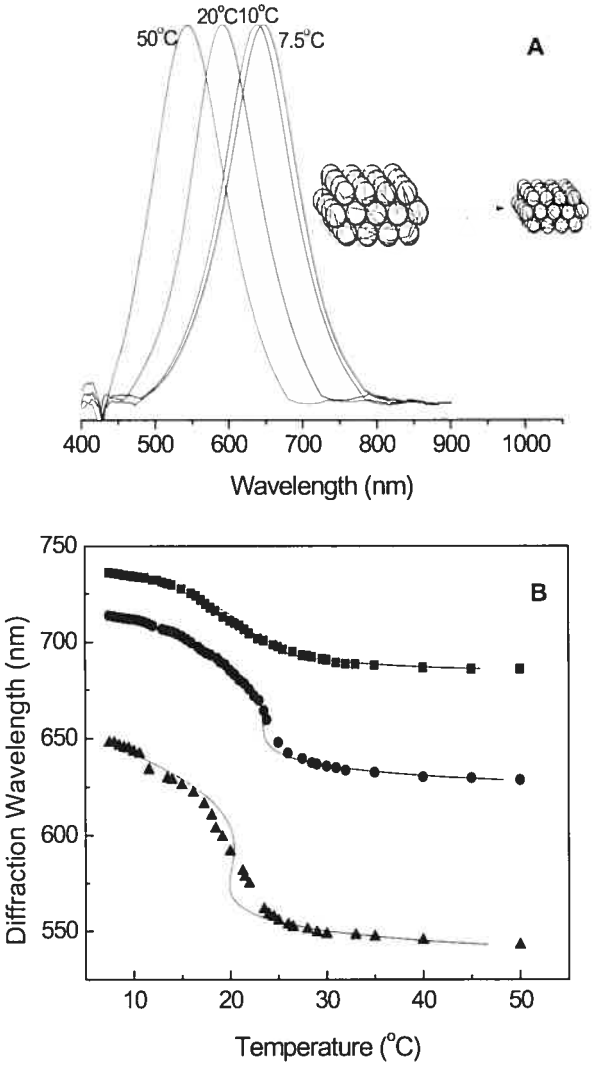

Figure 2.6 (A) Diffraction spectra of **PCCA3** at different temperatures; (B) diffraction wavelength as a function of temperature for PCCAs **1** (■), **2** (●), and **3** (▲). The data were fitted to eq. 7. The insert in (A) illustrates the response of PCCA (contraction in volume) upon heating.

The difference between the diffraction wavelengths at low and high temperatures ($\Delta\lambda$) is 50-100 nm, depending on the concentration of particles used to prepare the PCCA films (Table 2.2). At higher CCA concentrations, higher $\Delta\lambda$ was measured,

consistent with an increased compression between particles, and therefore increased stress release upon shrinkage. Finally, it is important to point out that the decrease in λ_{CCA}, λ_{PCCA} and λ_{20} with increasing concentration of CCA is also consistent with increasing particle compressions and a diminution of the lattice parameters.

In order to quantitatively characterize the phenomena observed, Flory's polymer solution and rubber elasticity theories were applied to these systems. The PCCA films were approximated as homogeneous mixtures, and the parameters were taken as average values for the particles and matrix polymers. The free energy is divided into mixing and elastic terms.[15-17] The mixing term of the gel system is treated by the Flory-Huggins polymer solution theory, and the corresponding free energy per unit volume, ΔG_m, is[15]

$$\Delta G_m / kT = (1-\phi)\ln(1-\phi) + \chi\phi(1-\phi) \tag{3}$$

where χ can be described as[24]

$$\chi = 0.34 + \frac{V_{H_2O}}{RT}(\delta_{H_2O} - \bar{\delta}_p)^2 \tag{4}$$

where k, R, T, ϕ, χ, V_{H_2O}, δ_{H_2O}, $\bar{\delta}_p$ are the Boltzmann constant, gas constant, the temperature, the polymer volume fraction, the Flory-Huggins polymer/solvent interaction parameter, the molar volume of water (1.8×10^{-5} m^3/mol), the solubility parameter of water (4.784×10^4 $J^{1/2}/m^{3/2}$),[25] and the average solubility parameter of the polymer, respectively. The polymer volume fraction, ϕ, can be substituted by $\phi = (\lambda_0/\lambda)^3$, where λ_0 is the diffraction wavelength that a PCCA films would display if it was fully dried without disrupting its ordering. However, it is impossible to dry PCCA films without disrupting their order and λ_0 therefore remains hypothetical.

In the Flory gel theory, the treatment of the elastic term is based on the rubber elasticity theory, which, in turn, is derived from the Gaussian chain model. The expression of the elastic free energy change, ΔG_E, is given by[16,17]

$$\frac{\Delta G_E}{kT} = \frac{3\nu_e}{4V_m}[(\frac{V}{V_m})^{2/3} - 1] \tag{5}$$

where ν_e/V_m is the cross-linking density in the network, V_m and V are the volumes of the fully relaxed gel and of the gel at equilibrium, respectively. Thus, $V/V_m = (\lambda/\lambda_m)^3$.

At equilibrium, the total free energy change must be zero:

$$\Delta G = \Delta G_m + \Delta G_E = 0 \qquad (6)$$

Thus, the relation between temperature and diffraction wavelength can be obtained from eqs. 3, 4, 5, and 6 and expressed in the following way:

$$(1-(\frac{\lambda_0}{\lambda})^3)\ln(1-(\frac{\lambda_0}{\lambda})^3)+(1-(\frac{\lambda_0}{\lambda})^3)(\frac{\lambda_0}{\lambda})^3(0.34+\frac{V_{H_2O}}{RT}(\delta_{H_2O}-\bar{\delta}_p)^2)+\frac{3v_e}{4V_m}((\frac{\lambda}{\lambda_m})^2-1)=0 \qquad (7)$$

Curve fitting of the diffraction wavelength versus temperature plots of the PCCA samples to eq. 7 was carried out. Table 2.3 lists the diffraction wavelength of hypothetical "dry" PCCA films λ_0, diffraction wavelength of relaxed PCCA gels λ_m, v_e/V_m, and $\bar{\delta}_p$ of PCCA in non-thermosensitive matrices (PAAm and PDMA) obtained by nonlinear fitting analysis. The values of λ_m indicate the point where the elastic free energy changes sign and are found to be 680 and 714 nm in PAAm and PDMA, respectively. At the fully relaxed state, λ equals λ_m, and $\Delta G_E = 0$. When the gel deswells, the diffraction wavelength λ is smaller than λ_m, so that the particles and matrix networks interact with each other with a positive chemical potential, resulting in a positive elastic free energy change. In the swollen state, when the diffraction wavelength λ is larger than λ_m, the particles and matrix networks interact with each other with a negative elastic free energy change. Therefore, the cross-linking density (v_e/V_m) obtained from eq. 5 have an unreasonable negative value. The absolute value of cross-linking densities, $|v_e/V_m|$, should be the "real" cross-linking density values (2.6, 0.86, 0.52 and 0.52 mol/m^3 for the PCCAs **1**, **2**, **3** and **4**, respectively). The PCCA prepared with a lower microsphere concentration has a higher cross-linking density than that prepared with a higher sphere concentration. It is therefore "as if" the elastic free energy change was determined by the matrix and not the microspheres. If we assume that the total volume of the composite does not change, the matrix has to expand to occupy the freed space when the microspheres shrink upon heating. In eq. 5, the volume V is related to the diffracted wavelength and therefore the volume of the microshperes, not to that of the matrix, which results in a negative sign for the cross-linking density. The average solubility parameters obtained from nonlinear fitting analysis are around

3~4 × 10^4 $J^{1/2}/m^{3/2}$, which are smaller than that of water and reasonable for polymers based on acrylamide.[25]

Table 2.3 Calculated λ_0, λ_m, v_e/V_m, $\bar{\delta}_p$ and correlation coefficient (R^2) of CCA embedded in non-thermosensitive matrices (PAAm (PCCAs **1-3**) and PDMA (**PCCA4**)).

Sample	λ_0 (nm)	λ_m (nm)	v_e/V_m (mol/m^3)	$\bar{\delta}_p$ (10^4 $J^{1/2}/m^{3/2}$)	R^2
PCCA1	676 ± 1	687 ± 1	− 2.6 ± 0.1	2.8 ± 0.1	0.99
PCCA2	609 ± 1	667 ± 2	− 0.86 ± 0.02	3.3 ± 0.1	0.99
PCCA3	511 ± 2	685 ± 12	− 0.52 ± 0.01	3.7 ± 0.1	0.98
PCCA4	469 ± 5	714 ± 20	− 0.52 ± 0.01	3.9 ± 0.1	0.99

ΔG_m, which depends on the volume fraction and temperature, and ΔG_E, which depends on the volume of the film, can be calculated from eqs. 3 and 5 by using the set of parameters obtained from the nonlinear fitting analysis. It was found that ΔG_E is positive for **PCCA3** and negative for **PCCA1** throughout the temperature range studied, which means that **PCCA1** was over-swollen whereas **PCCA3** was under-swollen. This is reflected by the diffraction wavelength changes of **PCCA3** ($\Delta\lambda$ = 105.0 nm) and **PCCA1** ($\Delta\lambda$ = 50.2 nm). For **PCCA2**, prepared at an intermediate CCA concentration, the ΔG_E can be negative or positive, depending on the volume of the film and the temperature. At lower temperatures, the film swells in water and has a negative elastic free energy component, while at higher temperatures, the film shrinks and expels some of its water content to reach a positive ΔG_E. Of course, the ΔG_E may be positive or negative, but the total free energy (ΔG) is zero with compensation from the mixing free energy.

The experimental data fit generally well with Flory-Huggins theories, but significant deviations were also observed for **PCCA3**. The high number of fitting parameters in eq. 7, in addition to the compression of the particles and the

interpenetration between the particles and the matrix, which became more significant at high concentrations, may be responsible of the deviation from the fitting approach.

2.4.4. PCCAs in thermosensitive matrices

Thermo-optical phenomena observed in the thermosensitive matrix-based PCCAs are more complex. Typically, double thermosensitivity is observed, owing to the thermosensitivity behaviors of both the particles (near 20 °C) and the matrix (32 °C for PNIPAM and 28 °C for PDEA).

Figure 2.7A shows the diffraction spectra of **PCCA7** at different temperatures. The relatively narrow and symmetrical diffraction spectra indicate a relatively high level of order with interplanar distances in the visible light region. Similar to what was observed for non-thermosensitive matrix PCCAs, the diffraction spectra of PCCAs **5-8** are blue-shifted with increasing temperature. Above 30 °C, the diffraction behavior vanishes, which, given the fact that the matrix is cross-linked, may indicate the disappearance of the refractive index mismatch between the matrix and the particles, although disruption of the ordered packing structure cannot be completely ruled out. Nevertheless, the phenomenon is reversible. The mass centers of the diffraction peaks are plotted against temperature for PCCAs **7**, **6**, and **5** (Figure 2.7B). Two distinctive regions are apparent, as expected from the two thermosensitive materials constituting these composites. The first region can be assigned to the VPT of the particles and the second region, at higher temperatures, corresponds to the transition of the matrix. Furthermore, the changes of the diffraction wavelength extend over a larger scale for PCCAs **5**, **6**, **7**, and **8** ($\Delta\lambda > 200$ nm) than for non-thermosensitive matrix-based PCCAs **1**, **2**, **3**, and **4** ($\Delta\lambda < 100$ nm) over the same temperature range (Table 2.2). However, the phenomena observed are not as sharp as in the case of non-thermosensitive matrix-based PCCAs, which may be due to strong particle/matrix interactions and the partial overlap of both thermosensitive steps. The VPTs resulting from the particles and the matrix may be mutually affected by the interpenetration of the polymer networks. The VPTs appear to be broad and shifted from the LCST of the polymers. We have observed a similar behavior in the case of core-shell doubly thermosensitive particles.[26]

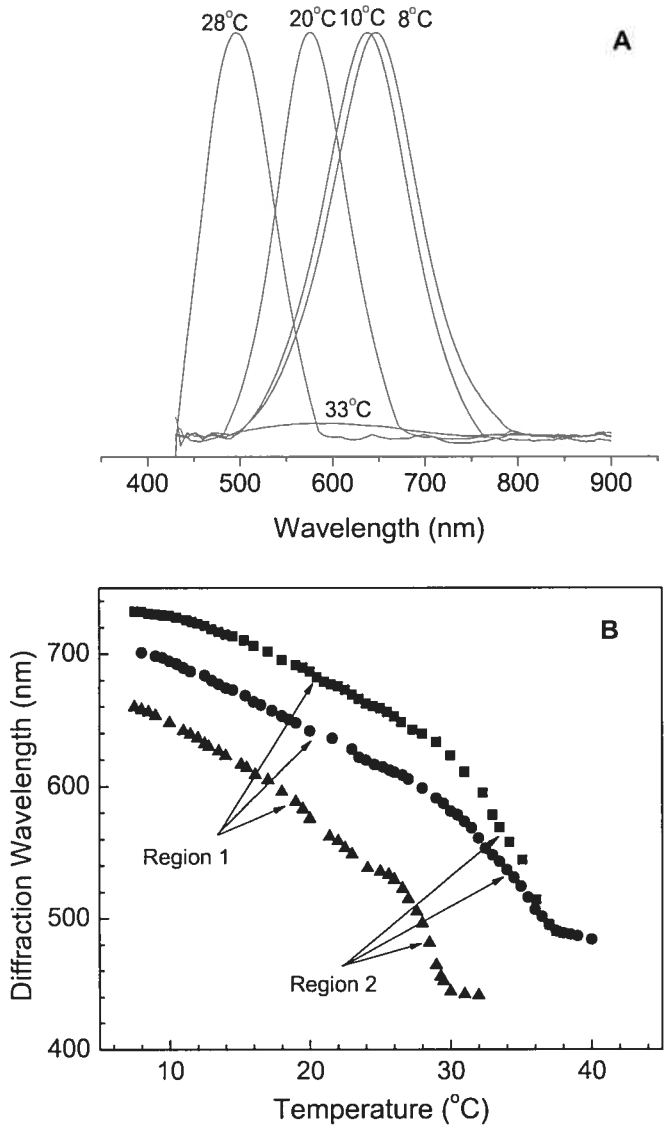

Figure 2.7 (A) Diffraction spectra of **PCCA7** at different temperatures; (B) diffraction wavelength versus temperature for PCCAs **5** (■), **6** (●), and **7** (▲).

2.4.5. Effects of ionic strength and pH

In order to demonstrate that other types of interactions, such as electrostatic or acid-base interactions, can also induce responsiveness in soft PCCAs, the effects of pH and ionic strength on their optical properties were investigated (Figure 2.8).

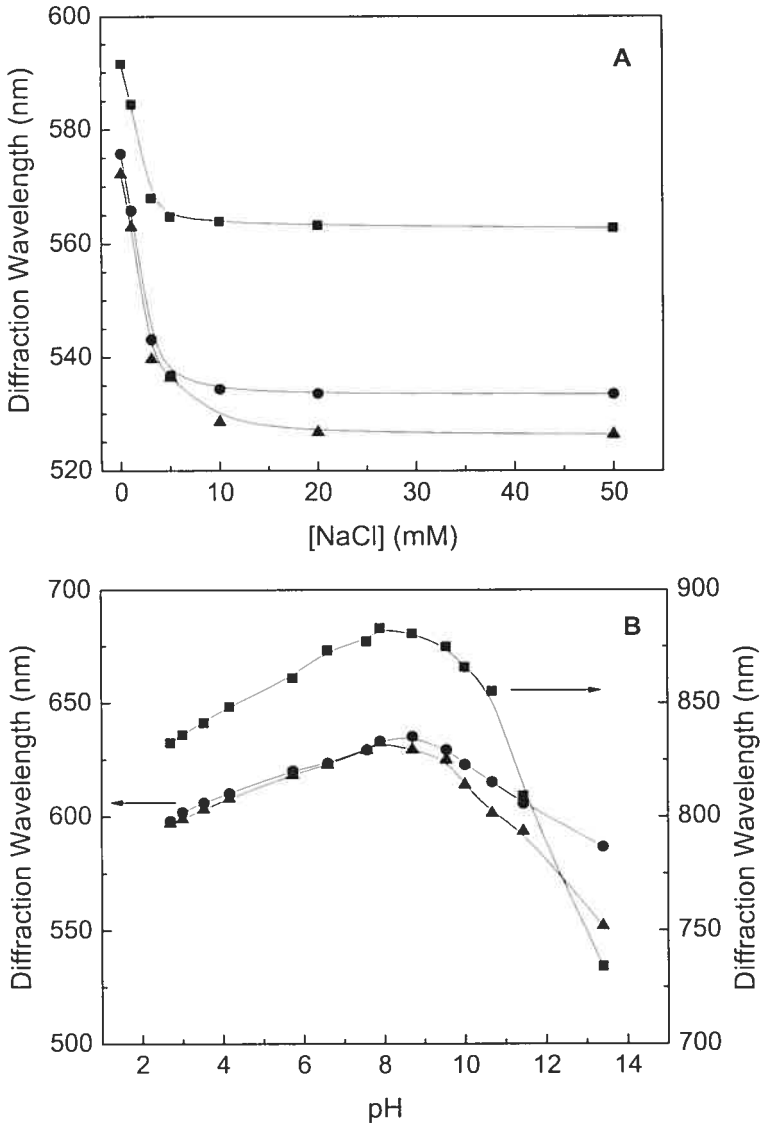

Figure 2.8 The dependence of the diffraction wavelength of PCCAs **3** (■), **7** (●), and **8** (▲) on (A) the ionic strength and (B) the pH (after partial hydrolysis of the amide groups), both measured at 20 °C.

Light diffraction spectra were recorded at different salt (NaCl) concentrations, and the diffraction wavelength maxima were plotted against salt concentrations for PCCAs **3**, **7**, and **8** (Figure 2.8A). The results show that increasing ionic strength induces the shrinkage of the PCCA films and blue-shifts the diffraction maxima until a maximum

shrinkage is reached. This effect, observed even at very low salt concentrations (< 5 mM), is thought to be due to a shielding of the polymer/solvent interactions (hydrogen bonding, dipole/dipole *etc.*) and subsequently deswelling of the PCCAs.[27] These results are consistent with those reported by Asher and co-workers for charged PS systems,[28] who interpreted the changes observed in terms of ionic free energy changes by adding a third component, ΔG_{ion}, in the treatment of eq. 6.

The pH response to PCCA films was evaluated after partial hydrolysis by immersing the samples for 3 minutes in a 1 N sodium hydroxide solution containing *N*,*N*,*N*',*N*'-tetramethylethylenediamine (TEMED, 10 wt%). During this treatment, some amide groups of the particle or the matrix may be hydrolyzed to form carboxyl groups. The samples were then immersed in solutions of different pH and diffraction spectra were recorded for partially hydrolyzed PCCAs **3**, **7**, and **8** (Figure 2.8B). The diffraction is monotonically red-shifted from pH 3 to 9,[28] while it is blue-shifted from pH 9 to 13.4. This pH dependence is due to the acid-base equilibria of the carboxyl groups. As the pH rises, the density of anions increases in the hydrogel, which generates a Donnan potential, increasing the osmotic pressure of the matrix, and indicating the swelling of the films and subsequent red shift of the diffraction peak. Above pH 9, the blue shift results from the increased ionic strength in the solution. The observation of pH sensitivity further demonstrates that simple post-functionalization of PCCAs allows chemical sensing.

2.5. Concluding remarks

A simple temperature cycling treatment of the thermosensitive and lightly cross-linked soft microspheres caused the spontaneous formation of well-ordered CCAs that display typical photonic phenomena. Such CCAs can then be embedded in both non-thermosensitive and thermosensitive matrices by photopolymerization of AAm, DMA, NIPAM, and DEA monomer solutions in the presence of a crosslinker at 5 °C. This affords thermosensitive and doubly thermosensitive PCCA films. For all PCCAs tested, a temperature increase results in a blue shift of the diffraction spectrum, due to the VPT of the embedded particles, in the case of non-thermosensitive matrices, or the VPTs of both particles and matrices, in the case of thermosensitive matrices. The free energy

change of the system is divided into two terms: the mixing (ΔG_m) and the elastic (ΔG_E) free energy changes. In the case of non-thermosensitive matrices, these two terms along with other parameters governing these systems can be calculated using non-linear fitting analysis, allowing a better understanding of the interplay of both mixing and elastic free energy changes in the thermo-optical phenomena observed.

The response of the PCCA films to changes in ionic strength and pH demonstrates the feasibility of PCCA-based chemical sensors and even more complex biological sensing devices. These systems based on soft hydrogels offer the advantage of simple colorimetric tests and easy optical detection. The presence of free hydroxyl functions in the microspheres would allow post-functionalization with a wide range of reagents and biological agents that may enable the recognition of molecules, proteins and DNA strands.

2.6. Acknowledgements

Financial support from FQRNT of Quebec, NSERC of Canada, and the Canada Research Chair program is gratefully acknowledged.

2.7. Notes and references

(1) L. E. Alexander, *X-ray Diffraction Methods in Polymer Science*; Wiley: New York, 1969.

(2) S. A. Asher, S. A. Alexeev, A. V. Goponenko, A. C. Sharma, I. K. Lednev, C. S. Wilcox, D. N. Finegold, *J. Am. Chem. Soc.* 2003, **125**, 3322.

(3) A. Chutinan, S. Noda, *Phys. Rev. B: Condens. Mater.* 2000, **62**, 4488.

(4) C. E. Reese, A. V. Mikhonin, M. Kamenjicki, A. Tikhonov, S. A. Asher, *J. Am. Chem. Soc.* 2004, **126**, 1493.

(5) R. J. Spry, D. Kosan, J. *Appl. Spectrosc.* 1986, **40**, 782.

(6) J. H. Holtz, S. A. Asher, *Nature* 1997, **389**, 829.

(7) J. M. Weissman, H. B. Sunkara, A. S. Tse, S. A. Asher, *Science* 1996, **274**, 959.

(8) P. N. Pusey, W. van Megen, *Nature* 1986, **320**, 340.

(9) J. D. Debord, S. Eustis, S. B. Debord, M. T. Lofye, L. A. Lyon, *Adv. Mater.* 2002,

14, 658.

(10) S. B. Debord, L. A. Lyon, *J. Phys. Chem. B* 2003, **107**, 2927.

(11) L. A. Lyon, J. D. Debord, S. Eustis, S. B. Debord, C. D. Jones, J. G. McGrath, M. J. Serpe, *J. Phys. Chem. B* 2004, **108**, 19099.

(12) S. Nayak, S. B. Debord, L. A. Lyon, *Langmuir* 2003, **19**, 7374.

(13) Z. Hu, X. Lu, J. Gao, *Adv. Mater.* 2001, **13**, 1708.

(14) J. Gao, Z. Hu, *Langmuir* 2002, **18**, 1360.

(15) P. J. Flory, *Principles of Polymer Chemistry*; Cornell University Press, Ithaca, NY, 1953; pp 432-594.

(16) P. J. Flory, *J. Chem. Phys.* 1977, **66**, 5720.

(17) J. E. Mark, B. Erman, *Rubberlike Elasticity, A Molecular Primer*; John Wiley & Sons: New York, 1988; pp 29-52.

(18) H. Y. Liu, X. X. Zhu, *Polymer* 1999, **40**, 6985.

(19) T. Hellweg, C. D. Dewhurst, E. Brückner, K. Kratz, W. Eimer, *Colloid Polym. Sci.* 2000, **278**, 972.

(20) J. H. Holtz, J. S. W. Holtz, C. H. Munro, S. A. Asher, *Anal. Chem.* 1998, **70**, 780.

(21) C. E. Reese, M. E. Baltusavich, J. P. Keim, S. A. Asher, *Anal. Chem.* 2001, **73**, 5038.

(22) H. Wolter, W. Storch, *J. Sol-Gel Sci. Tech.* 1994, **2**, 93.

(23) R. Guggenberger, W. Weinmann, *Am. J. Dent.* 2003, **13**, 82D.

(24) G. M. Bristow, W. F. Watson, *Trans. Faraday Soc.* 1958, **54**, 1731.

(25) J. Brandrup, E. H. Immergut, *Polymer Handbook*, 2nd ed., Wiley-interscience, New York, 1975, Sect. 4.

(26) Y. Chen, J. E. Gautrot, X. X. Zhu, *Langmuir* 2006, accepted for publication, DOI: 10. 1021/la0624945.

(27) I. Idziak, D. Avoce, D. Lessard, D. Gravel, X. X. Zhu, *Macromolecules* 1999, **32**, 1260.

(28) K. Lee, S. A. Asher, *J. Am. Chem. Soc.* 2000, **122**, 9534.

3. Synthesis and Characterization of Core-Shell Microspheres with Double Thermosensitivity*

3.1. Abstract

We have synthesized doubly thermosensitive core-shell microspheres composed of chemically cross-linked poly(*N*-*n*-propyl acrylamide-*co*-styrene) (P(nPA-*co*-S)) with different styrene contents as the core and linear poly(*N*,*N*-diethyl acrylamide) (PDEA), poly(*N*-isopropyl acrylamide) (PNIPAM), or poly(*N*-isopropyl methacrylamide) (PNIPMAM) as the shells. The morphologies and swelling properties of the core and the core-shell microspheres have been studied. The P(nPA-*co*-S) copolymers have a similar volume phase transition temperature regardless of the styrene content, indicating a two-layer structure in the microspheres with a PS-rich inner core and a PnPA-rich outer layer resulting from soap-free emulsion polymerization in water. Upon the addition of the second shell composed of linear thermosensitive polymers, the core-shell microspheres display a two-step shrinking behavior when heated. The P(nPA-*co*-S) core exhibits a volume phase transition temperature at 13-15 °C, while the shells of PDEA, PNIPAM, and PNIPMAM have volume phase transition temperatures at 28, 32, and 42 °C, respectively. The core-shell microspheres are composed of three layers and possess two volume phase transition temperatures.

3.2. Introduction

Stimuli-responsive polymeric hydrogels attract much research attention because of their versatility in fields such as controlled drug delivery,[1] chemical separation,[2] chemical and biological sensing,[3,4] catalysis,[5] enzyme and cell immobilization,[6] and color-tunable crystals.[7] Hydrogels of many *N*-substituted acrylamides were found to have a phase separation associated with changes in their properties upon heating above a certain lower critical solution temperature (LCST). Poly(*N*-propyl acrylamide) (PnPA),

---

* Paper accepted by *Langmuir*, November 2006. Authors: Yilong Chen, Julien E. Gautrot, and X. X. Zhu, DOI: 10. 1021/la0624945.

poly(*N*,*N*-diethyl acrylamide) (PDEA), poly(*N*-isopropyl acrylamide) (PNIPAM), and poly(*N*-isopropyl methacrylamide) (PNIPMAM) are typical examples of such polymers with LCSTs at 22, 28, 32, and 47 °C, respectively.[8,9] For potential applications of these materials as "smart" actuators and switches, a fast response is needed, for which several strategies have been explored. In particular, hydrogel microspheres (or microgels) have been developed because the response time of the microgel swelling has been reported to be short and proportional to the square of a linear dimension of the microspheres.[10] They were synthesized by classical emulsion polymerization techniques.[11,12]

A growing research interest has been devoted to responsive lattices that possess a more advanced architecture with multifunctionality. Numerous external stimulus-responsive core-shell or core-corona particles have been synthesized either to introduce spatially localized chemical functionalities to the particle,[13,14] or to graft thermosensitive layers to nonresponsive particles.[11,15-17] Many of the core-shell particles contain both a stimulus-responsive and nonresponsive component. Multiresponsive core-shell particles, which may have interesting applications, have also been reported recently.[18-23]

In this work, we report the preparation and properties of core-shell microspheres composed of a poly(nPA-*co*-S) core and shells of other thermosensitive polymers (PDEA, PNIPAM, and PNIPMAM) with three layers and two volume phase transition temperatures (VPTTs).

3.3. Experimental section

3.3.1. Materials

All chemicals were purchased from Aldrich. DEA and nPA were synthesized using a modified procedure described in the literature.[24,25] NIPMAM and potassium persulfate (KPS) were used without further purification. *N*,*N'*-Methylene bisacrylamide (BA) was recrystallized from methanol, and NIPAM was recrystallized from hexane and dried in vacuo prior to use. Styrene (S) was purified by distillation under reduced pressure. Water for all purposes was ion-exchanged to a resistance of 18.2 MΩ.cm (Milli-Q).

3.3.2. Preparation of P(nPA-*co*-S) cores

The P(nPA-*co*-S) cores were prepared via an emulsifier-free emulsion polymerization method. A mixture of S, nPA, and BA (Table 3.1) was dissolved in 235 mL of water in a 500-mL tri-necked round-bottom flask equipped with mechanical stirrer (350 rpm), nitrogen inlet and outlet. The monomeric solution was purged with nitrogen for 30 min at 70 °C to remove oxygen. Polymerization was initiated by adding 15 mL of an aqueous solution containing 0.12 g KPS. The reaction was allowed to proceed for 4 h at 70 °C under rigorous stirring. The resulting P(nPA-*co*-S) microspheres were purified by centrifugation and dialysis for 2 weeks.

Table 3.1. Experimental conditions for soap-free emulsion polymerization[a] in the preparation of mono-thermosensitive microspheres.

sample	nPA (g)	styrene (g)	$R_{h,10°C}$ (nm)	$R_{h,40°C}$ (nm)	α
PnPA5S95	0.113	1.976	102.9	101.7	0.954
PnPA25S75	0.565	1.560	335.8	223.7	0.298
PnPA50S50	1.130	1.040	344.5	175.9	0.132
PnPA75S25	1.695	0.520	505.8	252.7	0.120
PnPA90S10	2.034	0.208	482.5	244.0	0.119
PnPA	2.260	0	530.8	260.4	0.094

[a]0.0672 g of BA and 0.12 g of KPS were used in the preparation of all samples.

3.3.3. Preparation of core-shell microspheres

The thermosensitive shell layer was added using the above-prepared cores by a seed polymerization. The P(nPA-*co*-S) seed particles were polymerized for 4 h as described in the preparation of the P(nPA-*co*-S) cores and another aqueous solution (15 mL) containing 10 mmol of monomer (DEA, NIPAM, or NIPMAM) and KPS (0.06 g)

was added to the mixture in order to initiate the formation of the second shell. The polymerization was allowed to continue for 24 h under vigorous stirring (350 rpm). Polymerization may take place from the radicals still living on the seed particles.[15] The resulting shell layer are expected to contain mainly linear chains, since no cross-linker was added in the second step. The microspheres were purified by centrifugation and dialysis for 2 weeks to remove any linear chains that may be present.

3.3.4. Transmission electron microscopy (TEM)

To prepare an unstained specimen for TEM, the samples were diluted with deionized water. A drop of the sample was placed on a carbon-coated copper grid for 2 min. The excess solution was blotted with filter paper. After drying the grid samples in air, TEM images were taken with a Gatan Bioscan camera (model 792) set in the TEM instrument (Japan, JEOL JEM-2000FX) at an accelerating voltage of 80 kV.

3.3.5. Optical Transmittance

A Varian Cary (1 Bio) UV-visible spectrophotometer was used for transmittance measurements on samples of ca. 0.05 wt% at a heating rate of 1 °C/min. The cloud point was measured by monitoring the optical transmittance of a 500-nm light beam through a 1-cm sample cell referenced against distilled water at different temperatures.

3.3.6. Dynamic light scattering

Particle sizes were measured by DLS on a Brookhaven BI-200SM light scattering instrument set up with a Science/Electronics temperature controller (± 0.1 °C) and a 532-nm green JDS laser. The samples were allowed to equilibrate for 20 min at each temperature. Scattering light was detected at 90° with an integration time of 2 min and computed with a digital BI-9000AT correlator. In a DLS experiment the scattering light intensity autocorrelation function $g_I(t)$ is measured, which is related to the field autocorrelation function $g_E(t)$ by the Siegert relation[24,25]

$$g_I(t) = 1 + g_E^2(t) \quad (1)$$

For the case of purely translational motion,

$$g_E(t) = e^{-t/\tau} \qquad \frac{1}{\tau} = q^2 D \tag{2}$$

where τ is the relaxation time, q the scattering vector and D the diffusion coefficient. From D, a hydrodynamic diameter R_h is calculated using the Stokes-Einstein relation

$$D = \frac{kT}{3\pi\eta R_h} \tag{3}$$

which holds for noninteracting spheres. T denotes the temperature and η the viscosity of the solvent. In the case of polydisperse systems a relaxation time distribution $G(\ln \tau)$ must be used

$$g_E(t) = \int_{\ln \tau_{min}}^{\ln \tau_{max}} G(\ln \tau) e^{-t/\tau} d \ln \tau \tag{4}$$

which is obtained from $g_E(t)$ by CONTIN analysis.

3.4. Results and discussion

3.4.1. P(nPA-*co*-S) microsphere cores

Microspheres of P(nPA-*co*-S) with different styrene contents (Table 3.1) were synthesized by soap-free emulsion polymerization. TEM images of PnPA25S75 microspheres (Figure 3.1A) show a gray spherical ring around a dark core containing mainly polystyrene (PS). Figure 3.2A presents the optical transmittance data obtained for the P(nPA-*co*-S) cores with various styrene contents. It is particularly interesting to observe that the VPTT remains more or less constant, regardless of the change in the styrene content in the crosslinked microspheres. This is very different from the behaviors of the linear random copolymers of *N*-substituted acrylamides with styrene,[28] which showed a systematic decrease in their LCSTs with increasing styrene content. To verify this difference, we have prepared a linear copolymer of nPA containing 6.6 mol% styrene in methanol. A LCST at 6.7 °C was detected in water, similar to the previously published results.[28] This, together with the similar VPTT of pure PnPA, seems to indicate that the chemical composition of the thermosensitive outer layer of the spheres is pure PnPA.

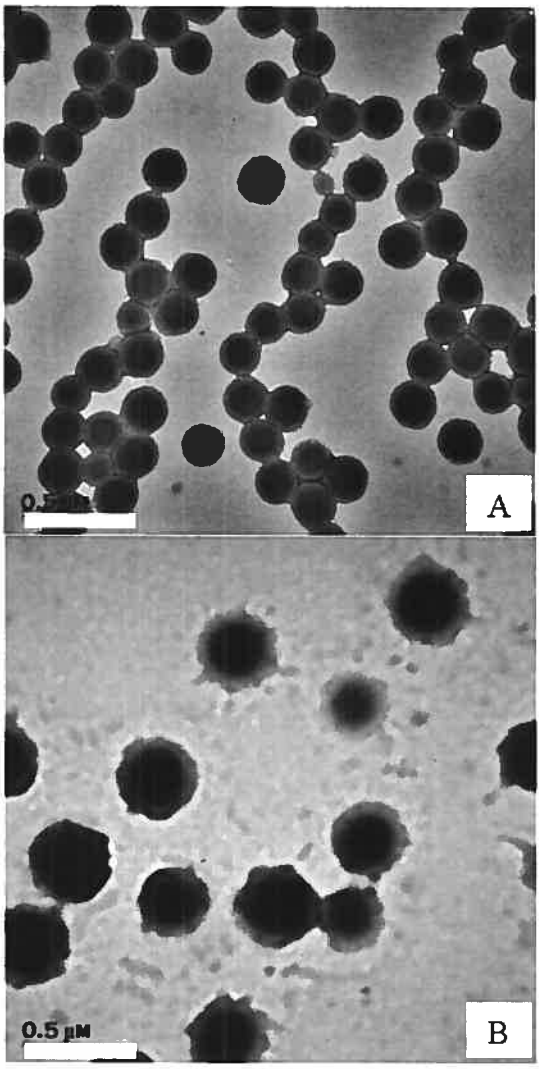

Figure 3.1. Transmission electron micrographs of (A) PnPA25S75 microspheres and (B) PnPA25S75-NIPAM core-shell microspheres. The numbers indicate the relative molar ratio of the comonomers.

Most of the styrene monomers were polymerized in the inner core of the microspheres. This is similar to the soap-free copolymerization of acrylamide with styrene in water studied by Kawaguchi and co-workers, who proposed a stepwise formation of the spheres.[29] The water-soluble initiator KPS first initiates the polymerization of water-soluble nPA. At this stage, styrene may be copolymerized but in smaller amounts despite its higher reactivity,[30] due to its higher hydrophobicity. The PnPA chains formed then act as polymeric stabilizers for the polymerization of the

styrene-rich cores, thus forming core-shell particles with PS cores and PnPA shells. Similarly, the small angle neutron scattering (SANS) study of the microspheres of PNIPAM-*co*-PS prepared by soap-free polymerization by Hellweg et al.[19] also indicated the formation of core-shell particles. Radical copolymerization of *N*-substituted acrylamides and styrene in organic solvent showed that the styrene content lowered the LCST remarkably due to its hydrophobicity,[30] while a hydrophilic comonomer such as acrylic acid shifted the LCST toward a higher temperature.[31] The results obtained with the present microspheres (Table 3.1) indicate that the chemical composition of the outer layer of the P(nPA-*co*-S) core is more or less constant (with a slightly lower VPTT than PnPA due to the presence of the styrene core), whereas the inner core, rich in styrene, is not thermosensitive. While the VPTTs of the microspheres are similar, Figure 3.2A also shows the evident difference in light transmittance of the microspheres at higher temperatures, which depends on the nPA content. Microspheres rich in styrene (such as PnPA5S95) are mainly non-thermosensitive, and thus their colloidal solutions did not show important temperature changes in their optical transmittance.

Figure 3.3A presents the size distribution of microspheres PnPA25S75, as measured by DLS. This typical example of the size distribution (half width of 40 nm) of the microsphere cores shows the low polydispersity of the particles synthesized, which is also confirmed by TEM. The temperature dependence of the hydrodynamic diameter is shown in Figure 3.4A, and important results are gathered in Table 3.1. It is clear that the hydrodynamic diameters decreased with increasing styrene content below VPTT of PnPA (at 10 °C), while above the VPTT of PnPA (at 40 °C), no clear trend is observed, possibly because of the shrinkage of the PnPA layer. Below the VPTT of PnPA, the higher the PnPA content, the larger the swollen network, whereas above the VPTT of PnPA, the effect of PnPA content on the hydrodynamic diameter is less trivial. From the hydrodynamic diameter, R_h, measured by DLS, the swelling ratio (α, Table 3.1) of the microspheres can be calculated from their volumes in the swollen and shrunk states by the use of the following equation:

$$\alpha = \frac{V_{\text{shrunk}}}{V_{\text{swollen}}} = \left(\frac{R_h^{313.2\text{K}}}{R_h^{283.2\text{K}}}\right)^3 \qquad (5)$$

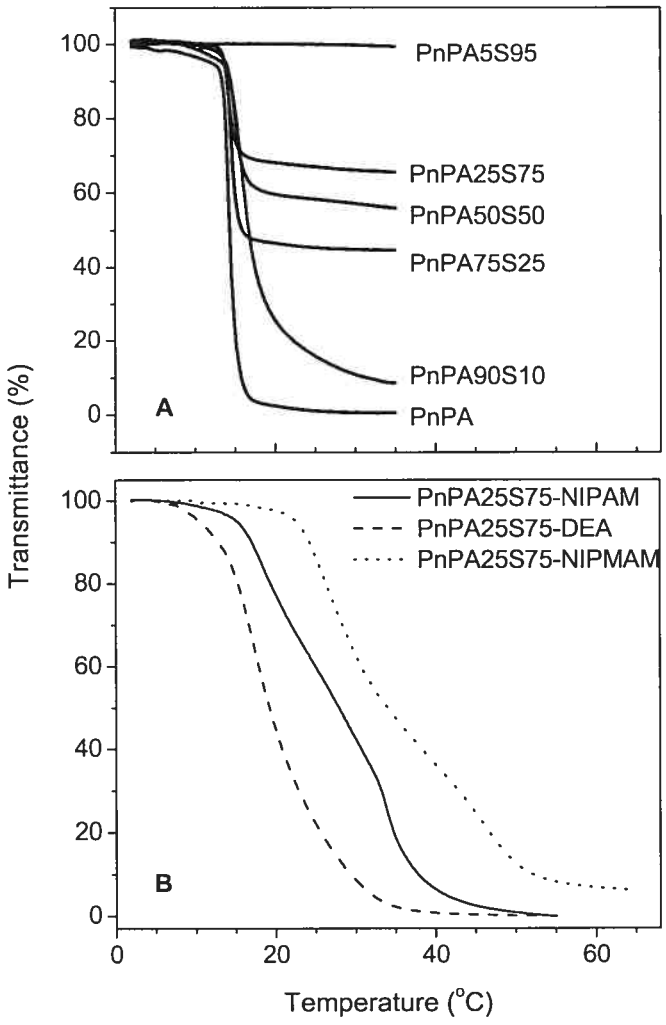

Figure 3.2. Optical transmittance of the solution of the microspheres as a function of temperature: (A) Mono-thermosensitive microspheres of P(nPA-*co*-S) with different polystyrene contents. (B) Doubly thermosensitive core-shell miscrospheres.

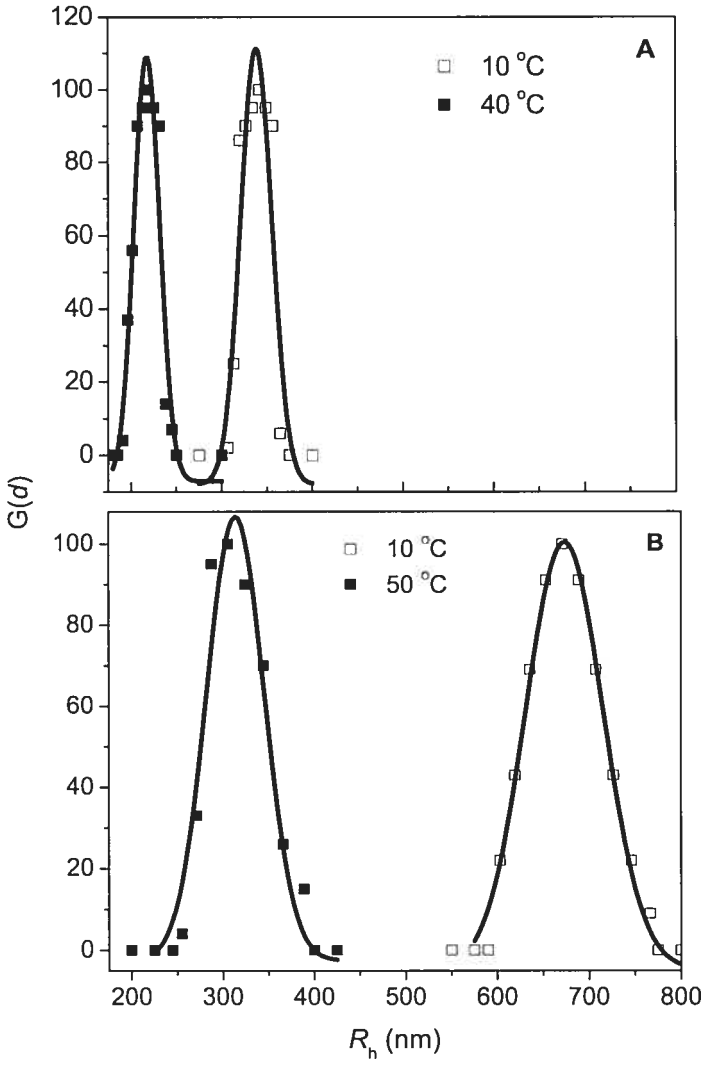

Figure 3.3. Size distributions of (A) PnPA25S75 and (B) PnPA25S75-NIPAM microspheres measured at different temperatures by DLS.

It seems that the values of α decrease with nPA content quickly to a constant value of ca. 0.12. At PS content of 95 mol%, no significant shrinkage of the microspheres with increasing temperature was observed. Controlling the PS content allows us to tune the hardness of the particles without changing their thermosensitive properties. The TEM, optical transmittance, and DLS results all indicate that P(nPA-*co*-S) microsphere cores have a structure with a PS-rich inner core and a PnPA-rich outer layer.

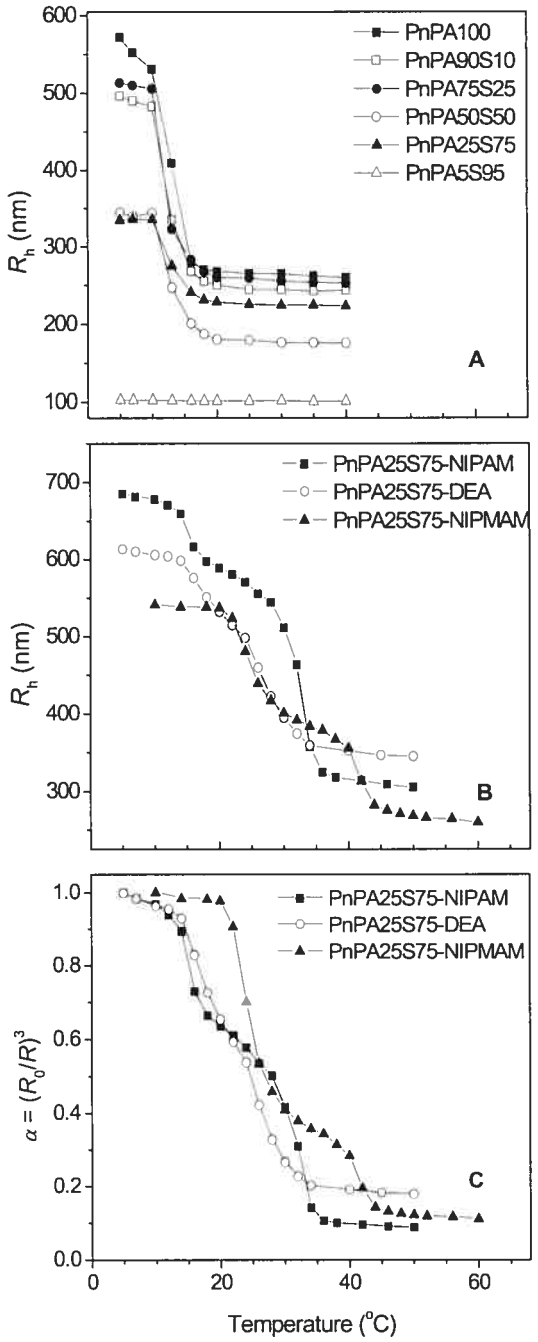

Figure 3.4. The variation of hydrodynamic diameters R_h or swelling ratios ($\alpha = (R_0/R_h)^3$) of the microspheres as a function of temperature: (A) mono-thermosensitive microspheres of P(nPA-*co*-S) with different PS contents; (B) doubly thermosensitive core-shell microspheres; (C) doubly thermosensitive core-shell microspheres.

3.4.2. Doubly thermosensitive core-shell microspheres

The second thermosensitive layer (PDEA, PNIPAM, and PNIPMAM) was formed on the P(nPA-*co*-S) particles (with nPA contents of 25 and 50 mol%) by seed polymerization. PS in the core helps to increase the contrast between the core and the shell when observed under TEM, since PS has a high electronic density, while poly(*N*-substituted acrylamide) has a lower electronic density. TEM images of PnPA25S75-NIPAM (Figure 3.1B) show a clear core-shell spherical structure, and the particle sizes are larger than those of the microsphere cores in Figure 3.1A. The DLS measurements show that the core-shell microspheres also have a narrow size distribution (half width of 70-80 nm, Figure 3.3B), even though the size distributions of the core-shell microspheres are wider than that of the core particles. The hydrodynamic diameters below and above the VPTT (at 10 and 50 °C, respectively) are both larger than those measured for their respective microsphere cores at similar temperatures. The increase in average diameter indicates that the shell has indeed been added to the core. The narrow size distributions of all the particles also suggest that the nucleation of new particles during shell addition is negligible. Should any linear polymers have been formed during seed polymerization, they may have entangled with the crosslinked matrix of the microspheres to form the core-shell structure, or they were removed during the purification process.

Temperature-dependent shrinking behaviors were studied by means of optical transmittance (Figure 3.2B) and DLS (Figure 3.4B), indicating quite clearly a two-step shrinkage upon rising the temperature as depicted in Figure 3.5. The first transition corresponds to the volume phase transition (VPT) of the thermosensitive outer layer of P(nPA-*co*-S) near 13-15 °C, while the second transition is attributed to the VPT of PDEA, PNIPAM, or PNIPMAM shells near 28, 32, or 42 °C, respectively, as illustrated by Figure 3.5. The thicknesses of the shells on PnPA50S50 seed particles were calculated to be 180, 235, and 175 nm for PDEA, PNIPAM, and PNIPMAM respectively, whereas the thicknesses of the shells on PnPA25S75 were estimated to be 275, 350, and 205 nm for PDEA, PNIPAM, and PNIPMAM shells, respectively. Furthermore, Figure 3.4B shows that the deswelling extent of the core-shell microspheres at the first VPTT compares well with that of the parent core particles. For

clarity of presentation, only the core-shell particles with a PnPA25S75 core are shown in Figures 3.2B and 4B, while other microspheres with different chemical compositions behaved similarly. These results indicate that core-shell microspheres can be obtained via a two-step aqueous seed polymerization. Interpenetrations may occur to some extent at the interface between seed and shell, resulting in a gradual decrease of the optical transmittance and hydrodynamic diameters. Such interpenetrations could be the reason that the VPTT of PnPA outer layer of the core microspheres was shifted to higher temperatures, which is more remarkable in the case of PnPA25S75-NIPMAM (Figure 3.4B) and PnPA50S50-NIPMAM (see Appendix). The extent of interpenetrations is expected to change depending on the core particles used and the nature of the thermosensitive monomer shell.

The swelling ratios of core-shell microspheres were calculated according to eq. 5 and shown in Figure 3.4C. Water expelled from the microspheres upon shrinking results in 8—90 vol% loss, compared to the fully swollen state. The two-step deswelling process depicted in Figure 3.5 is observed in Figure 3.4C with each step corresponding to the deswelling properties of the corresponding homopolymers. It shows that the PNIPAM and PNIPMAM shells of core-shell microspheres, which have larger volumes of expelled water (> 90 vol%), shrink more efficiently than others.

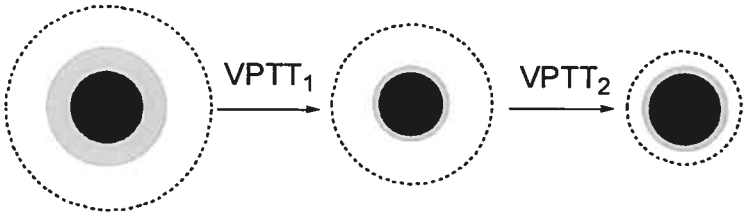

Figure 3.5. Schematic illustration of the response (change in size) of doubly thermosensitive core-shell microspheres to changes (increases) in temperature.

3.5. Concluding remarks

Doubly thermosensitive core-shell microspheres, which have a core of copolymer of nPA with styrene and a shell of N-alkyl (meth)acrylamide, can be prepared by a one-pot synthetic procedure. TEM images showed the formation of clear layered morphology in both the cores and the core-shell microspheres, and the stepwise swelling properties measured by DLS and optical transmittance further suggested the addition of soft shells that can respond to temperature changes. The microspheres have three layers and two VPTTs; the first VPTT remains more or less constant, while the second VPTT can be varied by the choice of polymers in the shell. The two-step swelling properties displayed by these microparticles may be useful in applications such as stepwise drug release and chemical separation.

3.6. Acknowledgments

Financial support from FQRNT of Quebec, NSERC of Canada, and the Canada Research Chair program is gratefully acknowledged. We thank Dr. Hojatollah Vali in FEMR of McGill University, for the assistance of the TEM observation.

3.7. References and notes

(1) Jeong, B.; Kim, S. W.; Bae, Y. H. *Adv. Drug Deliv. Rev.* **2002**, *54*, 37.

(2) Kawaguchi, H.; Fujimoto, K. *Bioseparation* **1998**, *7*, 253.

(3) Hu, Z. B.; Chen, Y. Y.; Wang, C. J.; Zheng, Y. D.; Li, Y. *Nature* (London) **1998**, *393*, 149.

(4) Van der Linden, H.; Herber, S.; Olthuis, W. *Sens. Mater.* **2002**, *14*, 129.

(5) Bergbreiter, D. E.; Case, B. L.; Liu, Y. S.; Waraway, J. W. *Macromolecules* **1998**, *31*, 6053.

(6) Guiseppi-Elie, A.; Sheppard, N. F.; Brahim, S.; Narinesingh, D. *Biotechnol. Bioeng.* **2001**, *75*, 475.

(7) Debord, J. D.; Eustis, S.; Debord, S. B.; Lofye, M. T.; Lyon, L. A. *Adv. Mater.* **2002**, *14*, 658.

(8) Platé, N. A.; Lebedeva, T. L.; Valuev, L. I. *Polym. J.* **1999**, *31*, 21.

(9) Iwai, K.; Matsumura, Y.; Uchiyama, S.; Silva, A. P. *J. Mater. Chem.* **2005**, *15*, 2796.

(10) Tanaka, T.; Fillmore, D. J. *J. Chem. Phys.* **1979**, *70*, 1214.

(11) Jones, C. D.; Lyon, L. A. *Macromolecules* **2000**, *33*, 8301.

(12) Xiao, X. C.; Chu, L. Y.; Chen, W. M.; Wang, S.; Xie, R. *Langmuir* **2004**, *20*, 5247.

(13) Duracher, D.; Sauzedde, F.; Elaissari, A.; Perrin, A.; Pichot, C. *Colloid Polym. Sci.* **1998**, *276*, 219.

(14) Zhu, G.; Elaissari, A.; Delair, T.; Pichot, C. *Colloid Polym. Sci.* **1998**, *276*, 1131.

(15) Matsuoka, H.; Fujimoto, K.; Kawaguchi, H. *Polym. J.* **1999**, *31*, 1139.

(16) Tsuji, S.; Kawaguchi, H. *Langmuir* **2004**, *20*, 2449.

(17) Tsuji, S.; Kawaguchi, H. *Macromolecules* **2006**, *39*, 4338.

(18) Jones, C. D.; Lyon, L. A. *Langmuir* **2003**, *19*, 4544.

(19) Hellweg, T.; dewhurst, C. D.; Eimer, W.; Kratz, K. *Langmuir* **2004**, *20*, 4330.

(20) Berndt, I.; Richtering, W. *Macromolecules* **2003**, *36*, 8780.

(21) Berndt, I.; Pedersen, J. S.; Richtering, W. *J. Am. Chem. Soc.* **2005**, *127*, 9372.

(22) Berndt, I.; Popescu, C.; Wortmann, F.; Richtering, W. *Angew. Chem., Int. Ed.* **2006**, *45*, 1081.

(23) Li, X.; Zuo, J.; Guo, Y.; Yuan, X. *Macromolecules* **2004**, *37*, 10042.

(24) Liu, H. Y.; Zhu, X. X. *Polymer* **1999**, *40*, 6985.

(25) Ulbrich, K.; Cech, L.; Kalal, J.; Kopecek, J. *Collec. Czech. Chem. Commun.* **1997**, *42*, 2666.

(26) Chu, B. *Laser light scattering, Basic principle and practice;* Academic Press, New York, 1991.

(27) Berne, B. J.; Pecora, R. *Dynamic light scattering;* Wiley, New York, 1990.

(28) Nichifor, M.; Zhu, X. X. *Polymer* **2003**, *44*, 3053.

(29) Ohtsuka, Y.; Kawaguchi, H.; Sugi, Y. *J. Appl. Polym. Sci.* **1981**, *26*, 1637.

(30) Bork, J. F.; Wyman, D. P.; Coleman, L. E. *J. Appl. Polym. Sci.* **1963**, *7*, 451.

(31) Kratz, K.; Hellweg, T.; Eimer, W. *Colloid Surf., A* **2000**, *170*, 137.

4. Biotin-Avidin-Based Biosensors

4.1. Introduction

Biotin-avidin interaction is widely utilized as a model pair in many applications ranging from purification techniques to modern diagnostics and targeted drug delivery. This methodology relies on the extremely high and specific affinity ($K_d \approx 10^{-15}$ M) between (strept)avidin and biotin.[1-9] This, together with biotin's role as an essential component in human biochemistry, has spurred the creation of a significant number of assay methods including microbiological, colorimetric, enzymatic, radiometric, electrochemical, and fluorescent approaches.[7-15] The most widely used detection method was that of Green's, which is a rapid and facile spectrophotometric procedure.[7,8,11] The fluorescence of fluorescein-labeled avidin can be enhanced with the addition of biotin.[16,17] This effect has been exploited to develop simple assays for avidin and biotin that are more sensitive and practical than the previous fluorimetric methods.[18]

Another approach for detection, which is more robust but not yet fully exploited, is the use of the structural and/or morphological changes in hydrogels/microspheres. Hydrogels/microspheres are soft materials that can be made to respond to external stimuli (electrical, thermal, optical or mechanical) and/or biological or chemical interactions.[19,20] These can trigger swelling or deswelling of the gel, and the changes in properties can be used to monitor the change in the environment. In this work, a thermosensitive microsphere will be biotinylated, which is then expected to respond to the addition of (strept)avidin in contact with the microsphere. Another approach for avidin detection is the use of PCCA. Functionalized PCCAs have been used as chemical and biological sensors, which are often called intelligent PCCA. Asher and co-workers have investigated extensively the intelligent PCCA for metal cation, glucose, creatinine in bodily fluids, and organophosphate sensing applications.[21-27] However, the intelligent PCCAs used previously were based on charged PS particles, which were hard and not compatible with the biological environment. Polymer hydrogels based on *N*-substituted acrylamides is a family of more hydrophilic polymers for biosensing applications.[28]

Biotin can be attached onto the matrix of the PCCA films. It is predicted that the light diffraction behaviors of the PCCA films can be changed by the addition of (strept)avidin.

4.2. Experimental section

4.2.1. Materials

All chemicals were purchased from Aldrich. DEA[29-31] and NAS[32,33] were synthesized using modified procedures described in the literature. Water for all purposes was ion-exchanged to a resistance of 18.2 MΩ.cm (Milli-Q). *N,N'*-Methylenebisacrylamide (BA) was recrystallized from methanol. Biotin (Aldrich), biotin hydrazide (Aldrich), avidin (Aldrich) and fluorecein labeled avidin (Vector Lab) were used as received.

Synthesis of DEA. *N,N*-Diethylacrylamide (DEA, Figure 4.1) was prepared from diethylamine and acryloyl chloride in dichloromethane. Acryloyl chloride (50 g, 0.54 mol) was slowly added in a dropwise manner into a solution of diethylamine (140 ml, 1.35 mol) in CH_2Cl_2 (400 ml) at 0 °C for 3 h. The solution was then stirred at room temperature overnight. The salt formed during the reaction was removed by filtration and washed thoroughly by CH_2Cl_2. After the removal of the solvent, the crude product was distilled under reduced pressure to yield colorless oil (84 % yields). ^{1}H- NMR ($CDCl_3$, ppm): δ = 6.45 (tri, 1H, *trans*-H in $=CH_2$), 6.23 (d, 1H, *cis*-H in $=CH_2$), 5.54 (m, 1H, =CH-), 3.30 (tetra, 4H, $2CH_2$), 1.06 (tri, 6H, $2CH_3$).

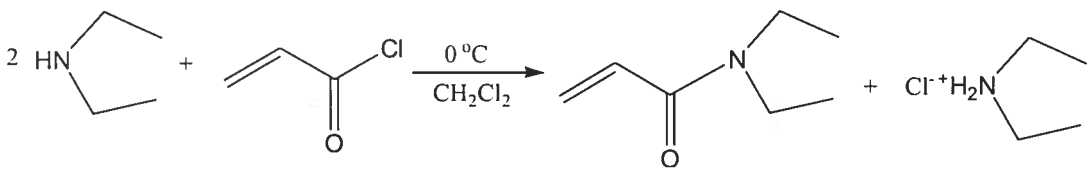

Figure 4.1. Synthesis of DEA.

Synthesis of NAS. *N*-Acryloxysuccinimide (NAS, Figure 4.2) was prepared according to literature procedure. Acryloyl chloride (8.5 ml, 1.2 eq.) was added

dropwise to a solution of *N*-hydroxysuccinimide (10 g, 86.9 mmol) and $(CH_3CH_2)_3N$ (14.6 ml, 1.2 eq.) in $CHCl_3$ (150 ml) over 30 min at 0 °C and stirred for another 30 min. The solution was washed successively with iced water and brine, and dried by anhydrous Na_2SO_4. Hydroquinon was added to the filtrate as a polymerization inhibitor and the solution was concentrated to a volume of 30-40 ml by a rotary evaporator. Ethyl acetate (10 ml) and hexane (80 ml) were added slowly with stirring. The solution was then kept in the refrigerator overnight. The crystals were filtered, washed successively 5 times with 200 ml of hexane/ethyl acetate (9 : 1) and 50 ml of hexane, and then dried to give a white solid in 84 % yield (12.3 g). ^{1}H- NMR (CD_3OD, ppm): δ = 6.75 (d, 1H, *trans*-H in $=CH_2$), 6.35 (t, 1H, *cis*-H in $=CH_2$), 6.20 (d, 1H, CH), 2.89 (s, 4H, $2CH_2$).

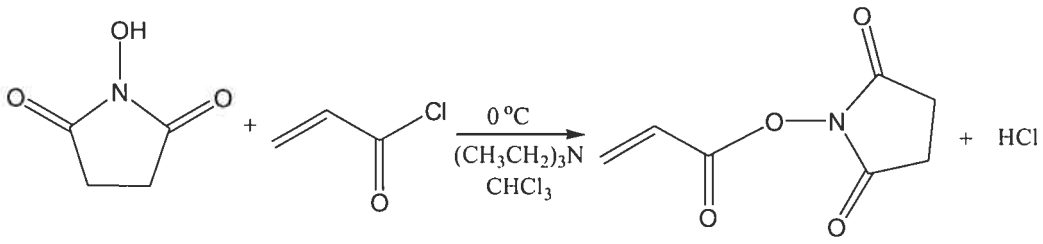

Figure 4.2. Synthesis of NAS.

Emulsion polymerization. In a typical procedure, the thermosensitive microspheres were prepared by traditional emulsion polymerization in 2 L tri-neck flask equipped with a mechanical stirrer (625 rpm). The monomers (71.3 mmol DEA, 7.9 mmol NAS), BA (1.2 mmol) and sodium dodecyl sulfate (SDS, 2.2 mmol) were added to 1 L of stirred milli-Q water followed by nitrogen purging for 30 minutes at reaction temperature (70 °C). Polymerization was initiated by adding a solution of potassium persulfate (KPS, 1.8 mmol in 15 ml of Milli-Q water) to the rigorously stirred mixture. The reaction was stopped after 4 h and allowed to cool down to room temperature before filtration of the resulting milky suspension through a 2.0 μm Millipore Isopore™ membrane filter (Sigma), and followed by centrifugation and dialysis for 14 days in a cellulose sack (Sigma, MW > 12,000) to purify the particles.

Biotinylation of microspheres.[34-37] Biotin hydrazide (20 mg, 0.077 mmol) was dissolved in 2 g (7.5 wt%) latex solution (90 mol% DEA and 10 mol% NAS) containing K_2HPO_4 buffer (0.1 M, pH 7.5). The reaction was carried out at room temperature for 24 h, followed by addition of ethanolamine (20 mg, 0.33 mmol) for 5 h to react with the excess of activated ester groups (Figure 4.3). The biotinylated microspheres were purified by dialysis for 14 days in a cellulose sack (Sigma, MW > 12,000).

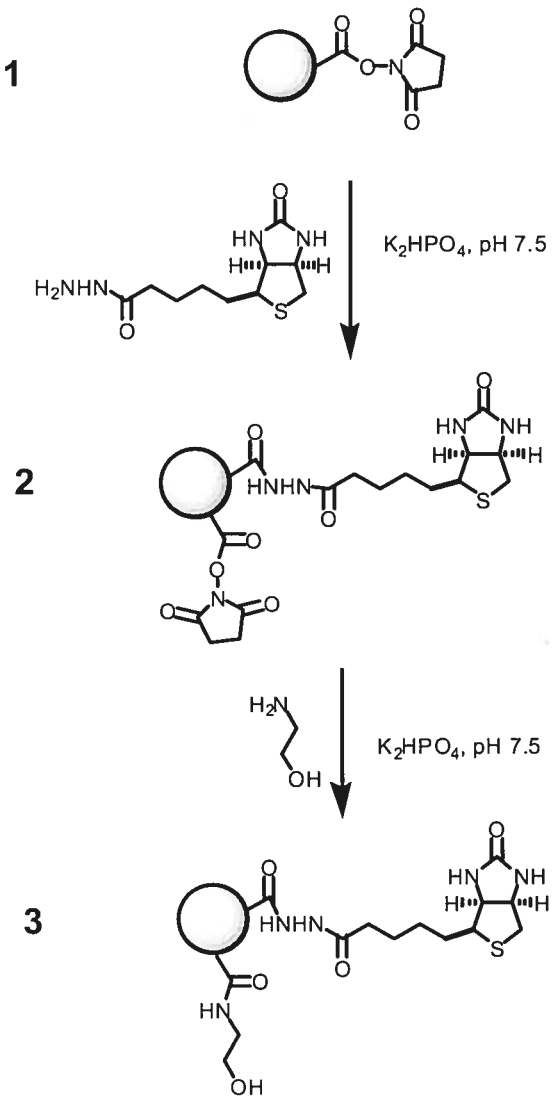

Figure 4.3. Biotinylation of microspheres (90 mol% DEA and 10 mol% NAS).

Preparation of biotinylated PCCA. CCAs were generated via a simple temperature cycling process (between 10 and 45 °C) of a solution of the thermosensitive microsphere (LCST around 20 °C) at the desired concentration. In a typical procedure, 2 g of a CCA latex, 100 mg of monomer (AAm), NAS (20 mg, 0.12 mmol) and 10 mg BA (cross-linker), and 50 µl diethoxyacetophenone (DEAP, Aldrich-Sigma, 10 vol% in DMSO) were placed in a chamber gasket (0.5 mm thickness, Molecular Probe) covered with a quartz slide at 5 °C, and subsequently illuminated with UV light (365 nm) for 10 h. The resulting films were washed with Mili-Q water for 7 days to remove chemical residues and swollen to their equilibrium state. By the reaction of biotin hydrazide (31 mg, 0.12 mmol) with succinimidyl ester groups in the matrix for 48 h in milli-Q water at room temperature, biotin was attached onto the matrix networks as illustrated in Figure 4.4.

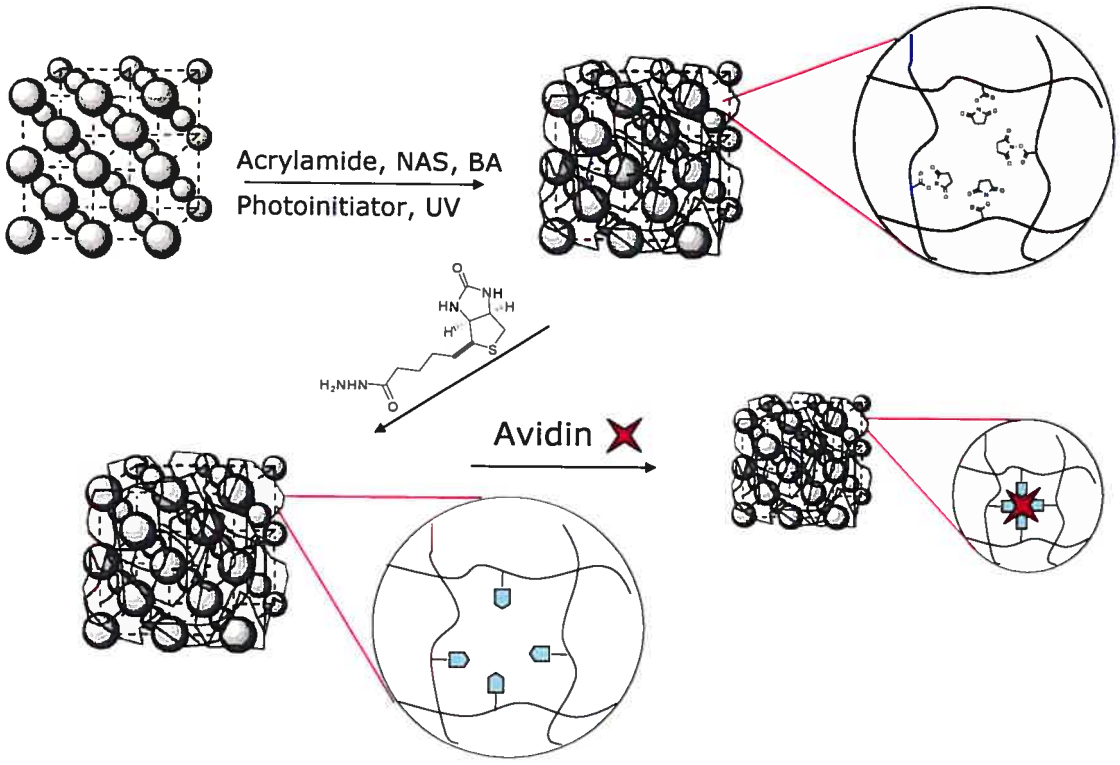

Figure 4.4. Preparation of avidin sensing PCCA.

4.2.2. Fluorescence measurements

Fluorescence spectra were measured on an FLS-900 (Edinburgh Instruments, UK) spectrofluorimeter. Fresh sample solutions were used in the fluorescence measurements. Stock solutions of biotin and biotinylated microspheres were prepared in Milli-Q water, and dilutions were made from this stock solution to get desired concentrations in sodium phosphate buffer solution (0.1 M, pH 7.5) containing 1 ml/L triton X-100 detergent. Stock solutions of fluorescein-labeled avidin (FLA) were prepared in methanol, and 500 µl aliquots of this stock solution were added to 5 ml of solutions to get a desired concentration (500 µg/L) for all the fluorescence measurements. The fluorescence spectra were excited at 495 nm with 5 nm slit and emitted at 520 nm with 5 nm slit. All the fluorescence spectra were recorded at room temperature.

To study competitive binding, FLA (500 µg/L) was added to a solution of biotin (8.4×10^{-8} M) or biotinylated microspheres (3.5 mg/L), and fluorescence spectra of fluorescein were recorded as a function of (strept)avidin concentrations in sodium phosphate buffer solution (0.1 M, pH 7.5) containing 1 ml/L triton X-100 detergent.

4.2.3. Visible light diffraction

Diffraction measurements were taken on a home-assembled spectrophotometer (Gamble Technologies USB2000, Figure 4.5) with wavelength coverage between 350-1000 nm, equipped with a tungsten halogen light source and a R200-7 VIS/NIR reflection probe (Ocean Optics). The prepared PCCA films were fragmented in order to have homogeneous samples in a UV cuvette. Temperature was controlled by using a circulating water bath. Temperature was measured by means of a thermocouple immersed in the solution (± 0.1 °C).

PCCAs diffract light and closely follow the Bragg diffraction law:

$$m\lambda = 2nd\sin\theta \qquad (1)$$

where m is the order of diffraction, λ is the wavelength of incident light, n is the refractive index of the suspension, d is the interplanar spacing, and θ is the glancing angle between the incident light and the diffracting crystal planes, oriented parallel to the crystal surface. Polychromatic light meeting the Bragg condition will be dispersed

with the longest wavelength meeting the Bragg condition diffracted at 90°. For back scattering $\sin\theta = 1$, a red beam (the longest wavelength) was obtained (Figure 4.6). As $\sin\theta$ decreases, the diffraction shifts to shorter wavelengths. By fixing the angle between the incident beam and the detector, the diffraction light shifts were monitored, when the PCCA shrinks or swells in response to environmental changes and stimulus responses.

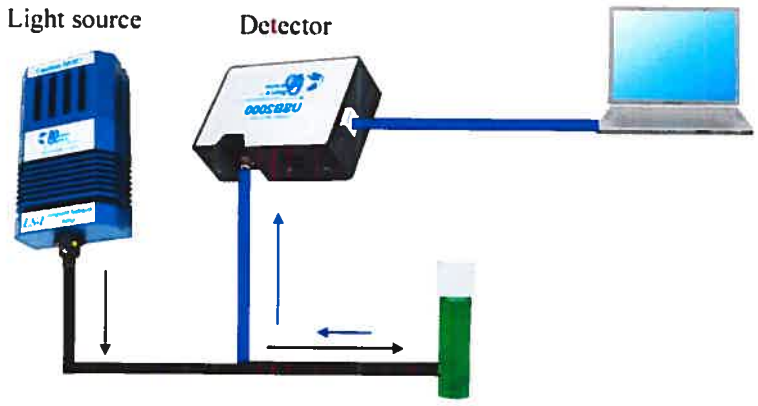

Figure 4.5. Home-assembled UV-visible light diffraction instrument.

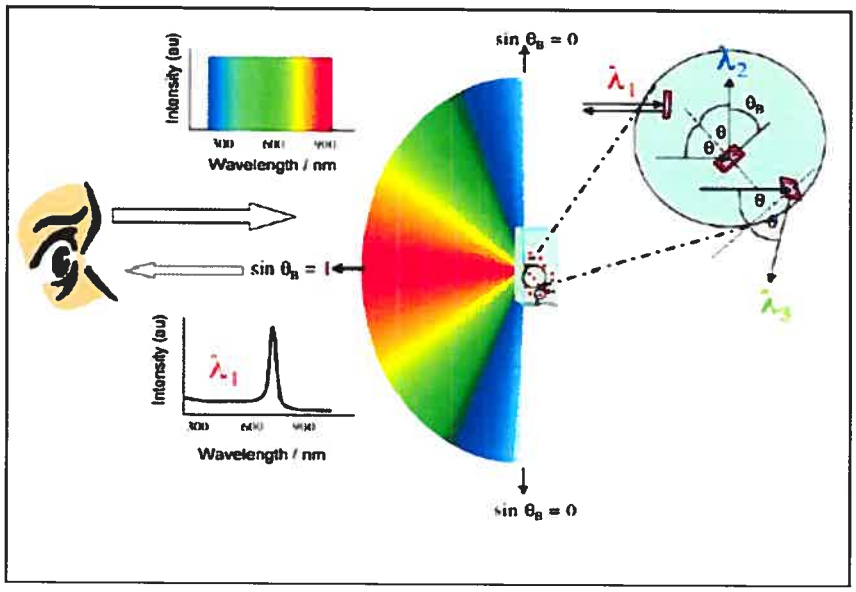

Figure 4.6. Light diffraction from PCCA (copied and modified from original in ref. 38).

4.3. Results and discussion

4.3.1. Biotinylation

Biotinylations of amines, thiols, aldehydes and carboxyl groups were widely used in the modifications of DNA, proteins, antibody and cell. *N*-Hydroxysuccinimide esters of biotins (NHS-biotin) are active esters that are extensively used in the modification of amino groups of proteins and cells, and in affinity chromatography. However, NHS-biotin is not a good candidate for the reasons of solubility in water and cost. Therefore, 10 mol% of NAS was used as a co-monomer in emulsion polymerization in order to introduce succinimidyl ester groups onto microspheres. Biotin was attached onto microsphere through the reaction of the succinimidyl ester groups of NAS and biotin hydrazide (Figure 4.3),[1-4] followed by an elimination of the remaining succinimidyl ester group on the microspheres by reacting with ethanolamine.

The starting microspheres (**1**), intermediate microspheres (**2**) and the final biotinylated microspheres (**3**) were analyzed by FTIR spectra with KBr film (Figure 4.7). The FTIR spectra clearly showed three strong absorption bands at 1810, 1782 and 1743 cm^{-1}, which were characteristic of the NAS group. Upon reaction with biotin hydrazide, these infrared bands became smaller, whereas a new shoulder band appeared at 3314 cm^{-1}, characteristic of the newly formed amide bond in microspheres **2** and **3** (see Figure 4.3 and Figure 4.7). Upon treatment with ethanolamine for 5 h, the three strong absorption bands of NAS group disappeared.

According to the literature, NAS reacts with amine to give *N*-oxysuccinimidyl anion (Figure 4.8), which has strong absorption at wavelength of 260 nm with absorbance 9700 $M^{-1}cm^{-1}$.[5] The absorption has a relative good linear relationship with NAS concentrations (Figure 4.9) in mixture solvent of methanol and water (MeOH : H_2O = 1 : 9) in the presence of isopropylamine (0.1 M). Principally, the amount of biotin attached on microspheres could be quantitatively estimated by measuring the amount of NAS on microspheres **1** (b = 0.341 mmol/g) and **2** (c = 0.175 mmol/g). The amounts of NAS on microspheres (**1** and **2**) could be calculated from the calibration plot (Figure 4.9) of NAS measured under the same conditions. Therefore, the amount of biotin attached on the microspheres, $a = b - c$ = 0.166 mmol/g, was obtained to be

0.166 mmol per gram dry microspheres indirectly by the amount of NAS losing upon reaction with biotin hydrazide by comparing the amounts of NAS of **1** with **2**.

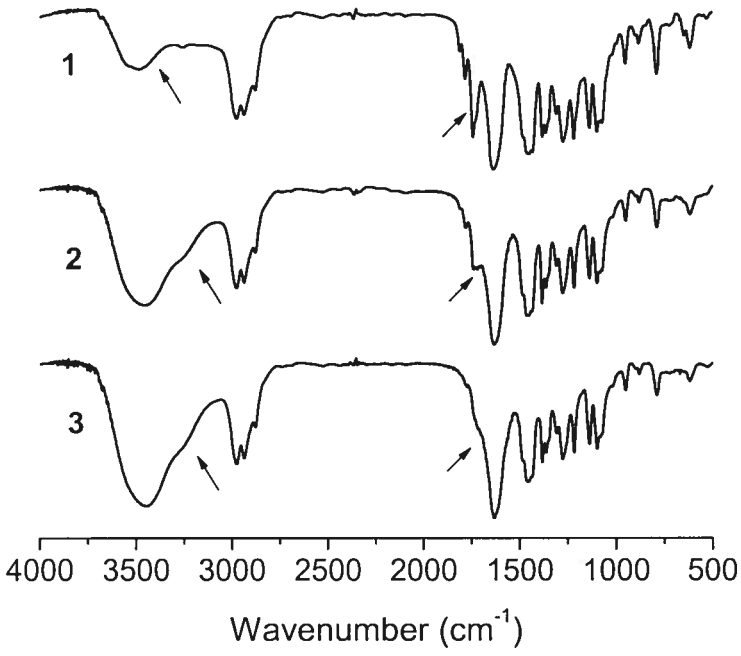

Figure 4.7. FTIR spectra of microspheres **1**, **2** and **3**.

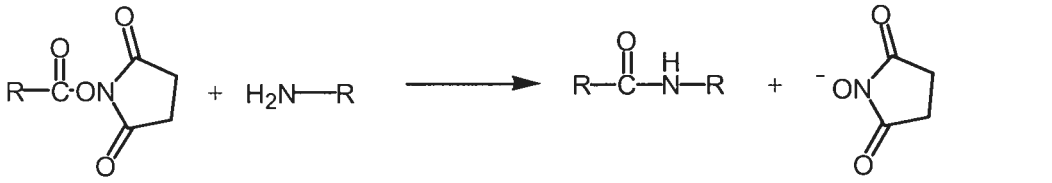

Figure 4.8. Quantification principle of NAS by UV.

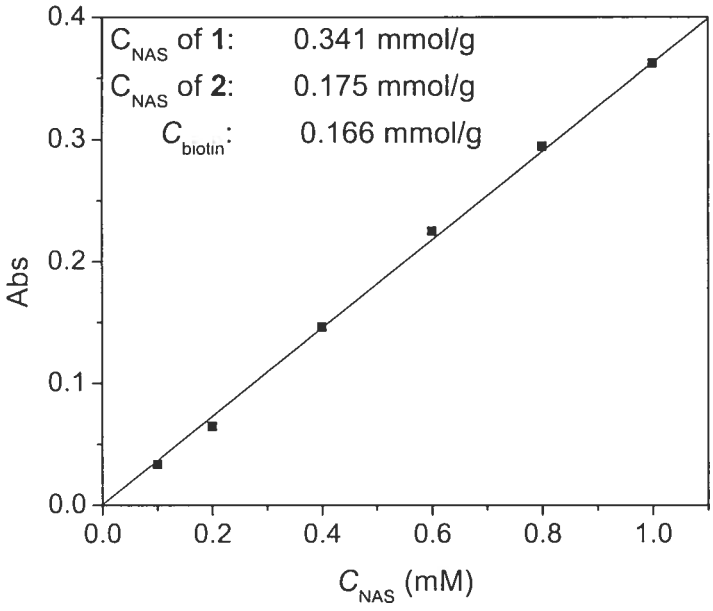

Figure 4.9. Calibration plot of NAS. From the calibration plot, the amounts of NAS group on microspheres **1** and **2** were measured and calculated to be 0.341 and 0.175 mmol per gram of dry microspheres, and thus the amount of biotin on the microsphere **3** can be measured and calculated to be 0.166 mmol per gram of dry microspheres.

4.3.2. Fluorescence measurements

Fluorescence spectra of fluorescein-labeled avidin were recorded at different concentrations of **3** (Figure 4.10A), and it showed that the fluorescence intensity was enhanced with an increase in the concentration of **3** in addition to a red shift of the spectra. The similar phenomena observed in our case have been observed previously in the case of free biotin.[16,17] It was explained that the microenvironment of fluorescein on avidin was changed because of biotin binding, resulting in a fluorescence enhancement. It also showed that the fluorescence of fluorescein-labeled avidin was enhanced in the presence of biotin to a plateau rapidly. Since there is significant change in the structure of avidin when biotin is bound,[11] the relatively large change in fluorescence of

fluorescein-labeled avidin was unexpected. However, biotin binding to dansyl avidin was found to lead to a 40 % reduction in emission intensity, which, together with fluorescence polarization evidence, suggested local displacement of dansyl groups into a more aqueous environment where they had greater rotational freedom and less interaction with the protein structure.[11] Such effects would be consistent with a biotin-induced increase in fluorescence of fluorescein groups attached to similar sites on avidin. Fluorescence intensities were plotted as a function of concentrations of free biotin, biotin attached on **3** and unbiotinylated microsphere (PDEA) in Figure 4.10B. One can notice that the fluorescence enhancement of fluorescein-labelled avidin in the case of biotinylated microspheres is smaller than that in the case of free biotin. This phenomenon suggests that the binding affinity between avidin and the biotin attached on the polymer microspheres is smaller than that between avidin and free biotin (10^{15} M^{-1}). Steric hindrance may be one cause and the swelling of the polymer networks could reduce the affinity between avidin and biotin as well. However, the binding constant cannot be estimated by nonlinear fitting analysis because the binding stoichiometric ratio is difficult to determine (1:1, 1:2, 1:3, or 1:4). Finally, one should point out that the presence of unbiotinylated microspheres (PDEA) cannot change the fluorescence intensity of fluorescein-labeled avidin.

The early work on avidin showed that the combination with biotin was very firm ($K = 10^{15}$ M^{-1}), which was treated as an irreversible binding for a long time. However, the dissociation constant by equilibrium dialysis with radioactive biotin gave an upper limit of 10^{-10} M. In later work, the dissociation constant was calculated from the ratio of the rate constants for the forward and reverse reactions, which was obtained from literature and presented in Table 4.1 at different pH values.[8,39,40] It suggested that the bound biotins could dissociate and exchange with the free one in the solution even it has such a high binding affinity for avidin. The high affinity of avidin for biotin, although ideal for specific labeling, is a disadvantage for affinity purifications of biotinyl enzymes, where it is not possible to substitute an iminobiotinyl residue. The binding affinity was reported to be weakened by selective oxidation of tryptophans of avidin, which was involved in the binding, with periodate and nitration ($K_d \approx 10^{-9}$ M).[11,41] In

our case, the binding affinity of avidin for biotin is predicted to be reduced by steric hindrance and the swelling of the polymer networks.

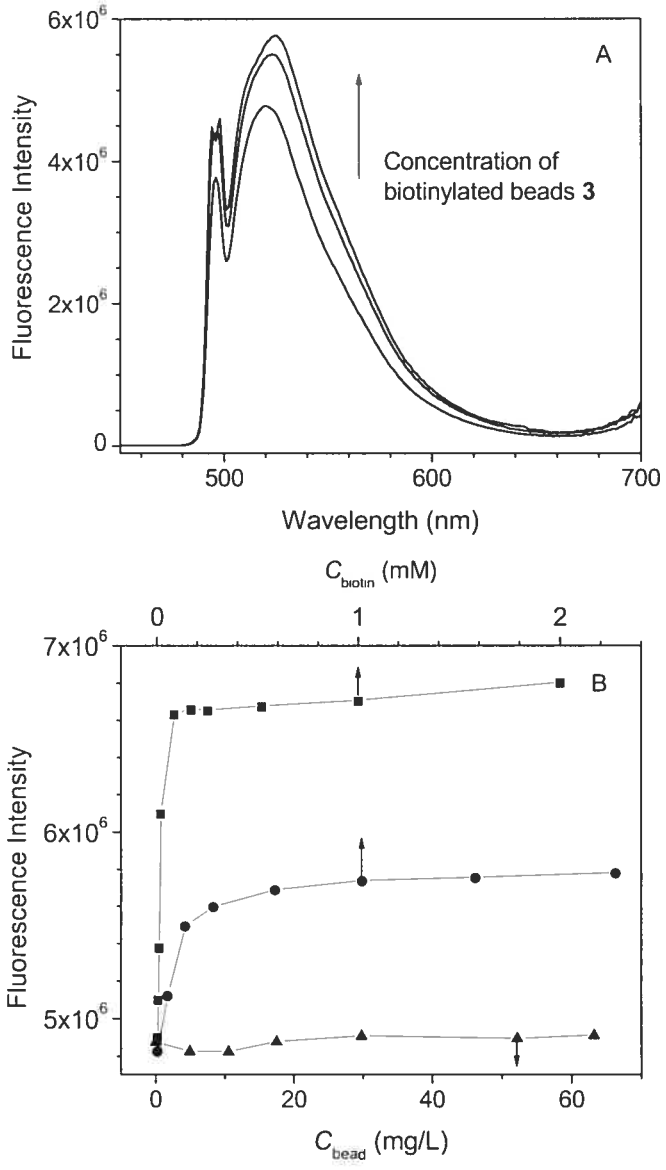

Figure 4.10. (A) Fluorescence spectra of fluorescein-labelled avidin (500 μg/L) in the presence of different concentrations of biotinylated microspheres (**3**); (B) plots of fluorescence intensity as a function of concentration of free biotin (■), biotin attached on **3** (●) and unbiotinylated microspheres made of PDEA (▲).

In order to further confirm the prediction, fluorescence studies of competition between fluorescein-labelled avidin and avidin (or streptavidin) for biotin attached on microspheres were carried out and presented in Figure 4.11. It shows that the fluorescence relative intensity decreases with the increase in concentrations of avidin (or streptavidin) as a result of the competition of avidin (or streptavidin) with fluorescein-labelled avidin. It suggests that the binding affinities of (strept)avidin and biotin attached on the particles are weakened. Furthermore, one can note that the fluorescence intensity decreases for high concentrations of streptavidin compared with similar concentrations of avidin. The reason is that the disassociation constant of streptavidin-biotin ($K_d \approx 4 \times 10^{-14}$ M) is larger than that of avidin-biotin ($K_d \approx 6 \times 10^{-16}$ M).

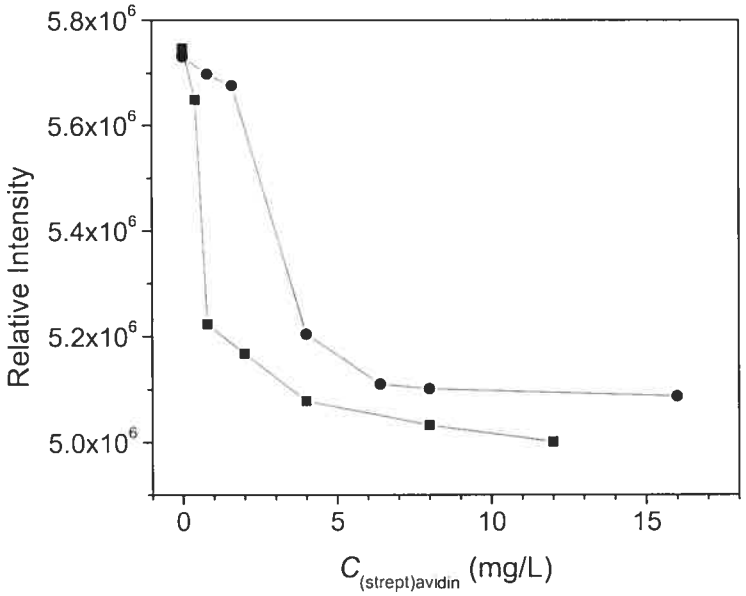

Figure 4.11. Fluorescence intensity of fluorescein-labeled avidin (500 μg/L) as a function of concentration of avidin (■), streptavidin (●) in the presence of biotinylated microspheres (47 nM of biotin on the microspheres).

Table 4.1. Dissociation rates (k) of avidin-biotin complexes[a] (copied and modified from original in ref. 8).

k and $t_{1/2}$	pH						
	1.7	2.0	3.0	5.0	7.0	9.2	10.5
Avidin							
k ($10^7 s^{-1}$)	--	200	9	0.9	0.4	--	--
$t_{1/2}$ (days)[b]	--	0.4	9	90	200	--	--
Streptavidin							
k ($10^7 s^{-1}$)	35	--	19	8.7	28	64	100
$t_{1/2}$ (days)[b]	2.3	--	4.2	9.2	2.9	1.25	0.8

[a]Exchange rates for streptavidin were measured at 25 °C using [^{14}C]biotin that had been purified by HPLC.[39] The exchange followed a simple first-order course apart from the first 10 % which, as with avidin, exchanged more rapidly. The methods and the results for avidin are taken from ref. 40.
[b] $t_{1/2}$ is half time of the dissociation between (strept)avidin and biotin.

4.3.3. Biotinylated PCCA

NAS was used as comonomers in the preparation of the matrix by photopolymerization to immobilize CCA (18.9 wt%) to make PCCA films, and followed by the reaction of biotin hydrazide with succinimidyl ester groups in the matrix, biotin were attached onto the matrix networks as illustrated in Figure 4.4. The light diffraction wavelengths in the absence and presence of avidin were recorded at 25 °C and plotted as a function of avidin concentration in Figure 4.12. It showed that the diffraction wavelength decreased with the increase in avidin concentration. It is interpreted that avidin acts as a cross-linker by binding with biotin molecules, and thus reducing the distance of the crystalline planes. However, the change of the diffraction wavelength ($\Delta\lambda \approx 25$ nm) is too small to be a sensing material by virtue of the particle-particle contacts and repulsion.

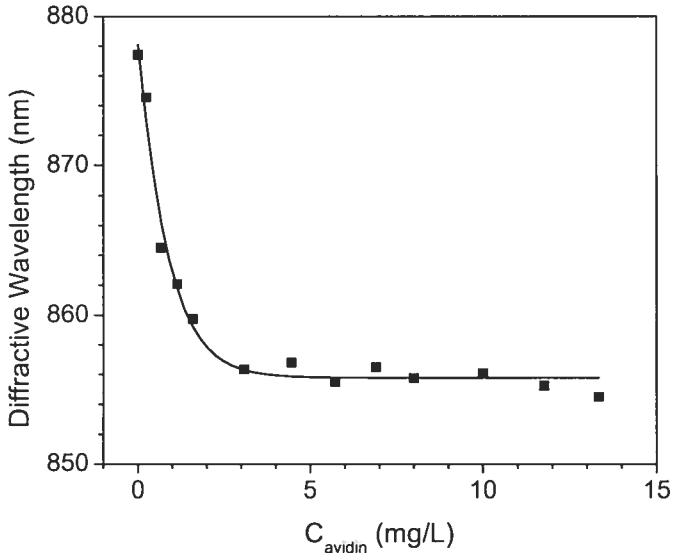

Figure 4.12. The diffraction wavelength of biotinylated PCCA as a function of avidin concentration.

4.4. Conclusions

Biotins were bonded chemically on lightly crosslinked, thermosensitive particles by reaction of biotin hydrazide with succinimidyl ester groups. Fluorescence studies of the binding interaction of fluorescein-labeled avidin and biotinylated microspheres showed that the binding affinity was weakened by the steric hindrance and the swelling of the polymer networks in comparison with the interaction of avidin with free biotin molecules. These phenomena indicate that the biotinylated microspheres can reversibly associate and disassociate with (strept)avidin. However, the size and degree of crosslinking of the biotinylated microspheres were not proper for use as a biosensor, because the DLS measurements showed (not shown) that the particle size does not vary with added avidin. To select appropriate microspheres for biosensing applications, different particle sizes, degrees of crosslinking and degrees of boitinylation of the microspheres should be tested.

For biotinylated PCCA, the change of the light diffraction wavelength upon the addition of avidin was too small to provide adequate sensing of the protein. In addition, the change in the wavelength of the diffracted light with temperature was much more significant than the response upon the addition of the protein. It is difficult to separate the contributions of the two stimuli causing in the same property (light diffraction wavelength, λ) of the system. A material that can manifest different changes in physical properties would be desirable. The diffraction intensity, rather than the wavelength, of the PCCA made of charged microspheres in nonthermosensitive matrices were reported to be enhanced by heating. The PCCA of charged thermosensitive microspheres (charged PNIPAM,[21] PDEA and PEA) in nonthermosensitive matrices (PAAm and PDMA), with no change in the diffraction wavelength with varying temperature, may be useful for such applications.

4.5. References

(1) Miller, B. T.; Collins, T. J.; Rogers, M. E.; Kurosky, A. *Peptides* **1997**, *18*, 1585.

(2) Veenman, C. L.; Reiner, A.; Honig, M. G. *J. Neurosci. Meth.* **1992**, *41*, 239.

(3) Petrie, C. R.; Adams, A. D.; Stamm, M.; Van Ness, J.; Watanabe, S. M.; Meyer, R. B. *Bioconjugate Chem.* **1991**, *2*, 441.

(4) Bernier, S.; Garreau, S.; Béra-Abérem, M.; Gravel, C.; Leclerc, M. *J. Am. Chem. Soc.* **2002**, *124*, 12463.

(5) Miron, T.; Wilchek, M. *Anal. Biochem.* **1982**, *126*, 433.

(6) Fucillo, D. A. *Biotechniques* **1985**, *3*, 494.

(7) Green, N. M. *Methods Enzymol.* **1970**, *18*, 418.

(8) Green, N. M. *Methods Enzymol.* **1990**, *184*, 51.

(9) Lin, H. J.; Kirsch, J. F. *Methods Enzymol.* **1990**, *62*, 287.

(10) Maliwal, B. P.; Lakowicz, J. *Biophys. Chem.* **1985**, *19*, 337.

(11) Green, N. M. *Adv. Protein Chem.* **1975**, *29*, 85.

(12) Veenman, C. L.; Reiner, A.; Honig, M. G. *J. Neurosci. Meth.* **1992**, *41*, 239.

(13) Petrie, C. R.; Adams, A. D.; Stamm, M.; Van Ness, J.; Watanabe, S. M.; Meyer, R. B. *Bioconjugate Chem.* **1991**, *2*, 441.

(14) Sutoh, K.; Yamamoto, K.; Wakabayashi, T. *J. Mol. Biol.* **1984**, *178*, 323.

(15) Bayer, E. A.; Zalis, M. G.; Wilchek, M. *Anal. Biochem.* **1985**, *149*, 529.

(16) Costello, S. M.; Felix, R. T.; Giese, R. W. *Clin. Chem.* **1979**, *25*, 1572.

(17) Guesdon, J. L.; Ternyck, T.; Avrameas, S. *J. Hisochem. Cytochem.* **1979**, *27*, 1131.

(18) Lin, H. J.; Kirsch, J. F. *Anal. Biochem.* **1977**, *81*, 442.

(19) Gehrke, S. H. *Adv. Polym. Sci.*, **110**, 81, 1993.

(20) Chen, G. H.; Hoffman, A. S. *Nature*, **1995**, *373*, 49.

(21) Holtz, J. H.; Asher, S. A. *Nature* **1997**, *389*, 829.

(22) Reese, C. E.; Mikhonin, A. V.; Kamenjicki, M.; Tikhonov, A.; Asher, S. A. *J. Am. Chem. Soc.* **2004**, *126*, 1493.

(23) Weissman, J. M.; Sunkara, H. B.; Tse, A. S.; Asher, S. A. *Science* **1996**, *274*, 959.

(24) Asher, S. A.; Alexeev, S. A.; Goponenko, A. V.; Sharma, A. C.; Lednev, I. K.; Wilcox, C. S.; Finegold, D. N. *J. Am. Chem. Soc.* **2003**, *125*, 3322.

(25) Walker, J. P.; Asher, S. A. *Anal. Chem.* **2005**, *77*, 1596.

(26) Holtz, J. H.; Holtz, J. S. W.; Munro, C. H.; Asher, S. A. *Anal. Chem.* **1998**, *70*, 780.

(27) Asher, S. A.; Sharma, A. C.; Goponenko, A. V.; Ward, M. M. *Anal. Chem.* **2003**, *75*, 1676.

(28) Hu, Z.; Lu, X.; Gao, J. *Adv. Mater.* **2001**, *13*, 1708.

(29) Liu, H. Y.; Zhu, X. X. *Polymer* **1999**, *40*, 6985.

(30) Idziak, I.; Avoce, D.; Lessard, D.; Gravel, D.; Zhu, X. X. *Macromolecules* **1999**, *32*, 1260.

(31) Shea, K. J.; Stoddard, G. J.; Shavelle, D. M.; Wakui, F.; Choate, R. M. *Macromolecules* **1990**, *23*, 4497.

(32) Pollack, A.; Blumenfeld, H.; Wax, M.; Baughn, R. L.; Whitesides, G. M. *J. Am. Chem. Soc.* **1980**, *102*, 6324.

(33) Baek, M. G.; Roy, R. *Macromol. Biosci.* **2001**, *1*, 305.

(34) Miller, B. T.; Collins, T. J.; Rogers, M. E.; Kurosky, A. *Peptides* **1997**, *18*, 1585.

(35) Veenman, C. L.; Reiner, A.; Honig, M. G. *J. Neurosci. Meth.* **1992**, *41*, 239.

(36) Petrie, C. R.; Adams, A. D.; Stamm, M.; Van Ness, J.; Watanabe, S. M.; Meyer, R. B. *Bioconjugate Chem.* **1991**, *2*, 441.

(37) Bernier, S.; Garreau, S.; Béra-Abérem, M.; Gravel, C.; Leclerc, M. *J. Am. Chem. Soc.* **2002**, *124*, 12463.

(38) Reese, C. D.; Baltusavich, M. E.; Keim, J. P.; Asher, S. A. *Anal. Chem.* **2001**, *73*, 5038.

(39) Garlick, R. K.; Giese, R. W. *J. Biol. Chem.* **1988**, *263*, 210.

(40) Green, N. M.; Toms, E. J. *Biochem. J.* **1973**, *133*, 687.

(41) Morag, E.; Bayer, E. A.; Wilchek, M. *Biochem. J.* **1996**, *316*, 193.

5. Conclusions

5.1. Preparation of microspheres

Thermosensitive microspheres were synthesized by emulsion polymerization. The particle size can be controlled by varying the concentration of surfactant (SDS) and monomers. By controlling the size, microspheres with various swelling ratios can be prepared to meet the needs of various applications such as controlled drug delivery, chemical separation, chemical and biological sensing, catalysis, enzyme and cell immobilization, and color-tunable crystals.

Doubly thermosensitive core-shell microspheres, which have a core of copolymer of nPA with styrene and shells of thermosensitive poly(*N*-alkyl (meth)acrylamide, can be synthesized in a one-pot soap-free emulsion polymerization. TEM images showed clear core-shell morphology in both cases of the core and the core-shell microspheres. This has been confirmed by the stepwise swelling properties. These microspheres having three layers and two LCSTs may prove to be useful in applications of stepwise drug release and chemical separation.

5.2. CCA formation by microspheres

The soft microspheres with no surface charges can be packed into an ordered CCA as a result of particle-particle interactions, which is different from formation mechanism of PCCA made of charged microspheres. The ordered packing of CCA causes the diffraction of light of a certain wavelength depending on the interparticle distance, which may be utilized for sensing applications.

5.3. Polymerized CCAs and their characteristics

CCA can be successfully embedded/immobilized in crosslinked nonthermosensitive (PAAm and PDMA) and thermosensitive (PDEA and PNIPAM) matrices by the photopolymerization of a solution of monomers with CCAs. The interpenetration of the thermosensitive microspheres and the nonthermosensitive

matrices can cause volume changes of the nonthermosensitive matrices of the films upon a change in temperature, which can be theoretically described by Flory's gel theories. The PCCA films can respond to changes in ionic strength and pH, which demonstrates the feasibility of PCCA-based chemical sensors and may help in the design of useful biological sensing devices. The modification of the PCCA films via post-functionalization should enable the detection of a wide range of analytes by simple colorimetric tests. Therefore, these soft hydrogel-based composites appear to be good candidates for biosensing applications and offer the advantage of easy optical detection. Moreover, the presence of free hydroxyl functions in the microspheres would allow post-functionalization with a wide range of reagents and biological agents that would enable the recognition of molecules, proteins and DNA strands.

5.4. Biotinylation and sensing technology

Biotin has been incorporated into the microgel particles. Fluorescence measurements suggested that the biotinylated microspheres can reversibly bind and release (strept)avidin, which made the microspheres reusable. However, the response of particle size was not adequate for biosensing applications. Thus, further studies may focus on the effects of particle size, degree of crosslinking and degree of biotinylation of the microspheres. Hopefully, the microspheres with optimized properties can respond upon the addition of (strept)avidin (Figure 5.1).

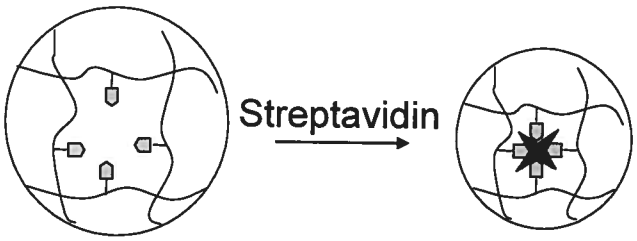

Figure 5.1. Schematic illustration of (strept)avidin responsive microspheres.

PCCA films of uncharged microspheres were also biotinylated and studied. The change of diffraction wavelength upon the addition of (strept)avidin has been studied. The PCCA films of thermosensitive uncharged microspheres are not ideal for bio-sensing applications because of the small change in the diffraction wavelength. The reason is that the microspheres are compressed too much in the PCCA films, which makes any change in the interparticle distance difficult. More space between the microspheres in PCCAs would be needed for sensing applications. Smaller particles and PCCAs of charged thermosensitive microspheres, which formed CCA in solution by electronic repulsion, might be suitably bio-functionalized for bio-sensing applications.

Even though significant advances have been made in polymer-biomolecule conjugation and biosensing, many challenges still remain for the development of versatile polymeric biosensors. This is an initiating study of bio-sensing materials based on thermosensitive microspheres. Our study offers a better understanding of the soft polymeric microspheres. The use of these thermosensitive polymers for the development of functional polymer materials should be further explored.

APPENDICES

A. Appendix of Chapter 2

The eq. 7 in chapter 2 can be expressed as the following:

$$-\frac{1}{T}\frac{V_{H_2O}}{R}=\frac{(1-(\frac{\lambda_0}{\lambda})^3)\ln(1-(\frac{\lambda_0}{\lambda})^3)+\frac{3v_e}{4V_m}((\frac{\lambda}{\lambda_m})^2-1)}{(1-(\frac{\lambda_0}{\lambda})^3)(\frac{\lambda_0}{\lambda})^3(\delta_{H_2O}-\overline{\delta}_p)^2}-\frac{0.34}{(\delta_{H_2O}-\overline{\delta}_p)^2} \qquad (A1)$$

where V_{H_2O} is 1.8×10^{-5} m^3/mol and δ_{H_2O} is 4.784×10^4 $J^{1/2}/m^{3/2}$ as described on page 37, λ is an independent variable, $-\frac{1}{T}\frac{V_{H_2O}}{R}$ is the dependent variable, and λ_0, λ_m, v_e/V_m, $\overline{\delta}_p$ are parameters that were left free to vary during the curve fitting procedure. The fittings were performed by the use of OriginPro 7.5 until reasonable correlation coefficients (R^2) and errors of the fitting parameters were obtained. The data are shown with the fitted curves in Figure A1. The fitting results are shown as λ -T curves in Figure 2.6B on page 36. The differentiation curves of the data in Figures 2.6B and 2.7B are shown in Figures A2 and A3 to show the transition temperatures more clearly.

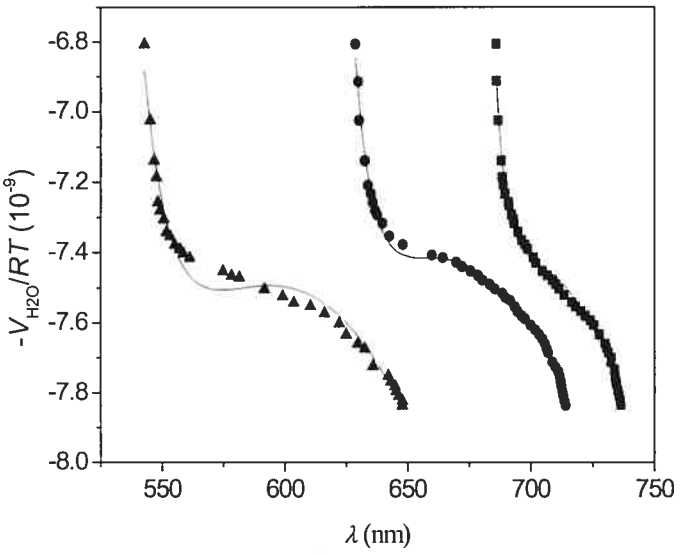

Figure A1. The fitting curves of λ versus $-\frac{1}{T}\frac{V_{H_2O}}{R}$.

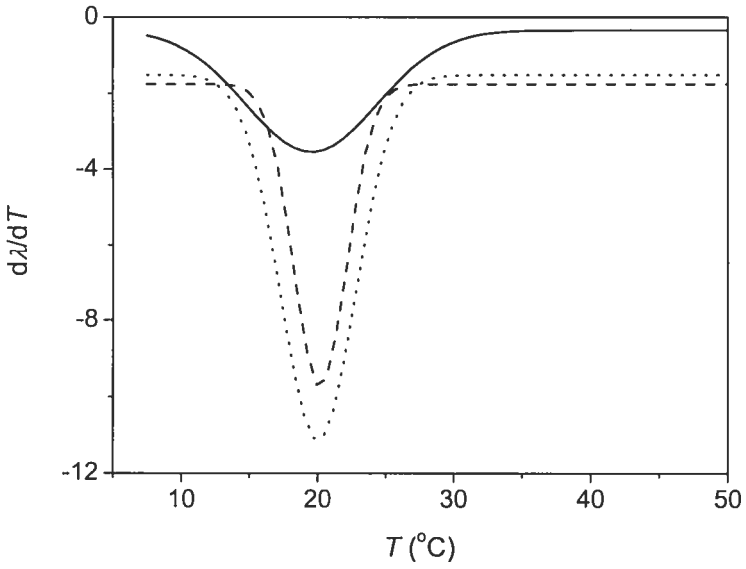

Figure A2. The differentiating curves of data in Figure 2.6(B) for PCCAs **1** (Solid), **2** (Dash), and **3** (Dot).

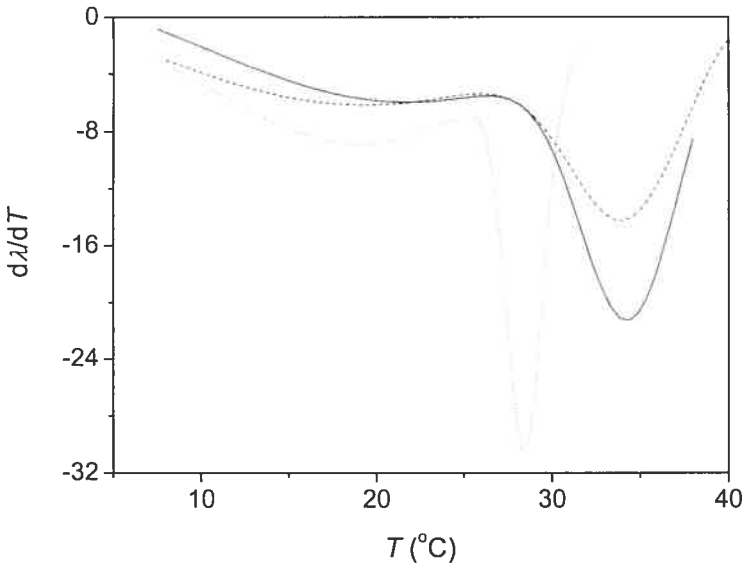

Figure A3. The differentiating curves of data in Figure 2.7(B) for PCCAs **5** (Solid), **6** (Dash), and **7** (Dot).

B. Appendix of Chapter 3

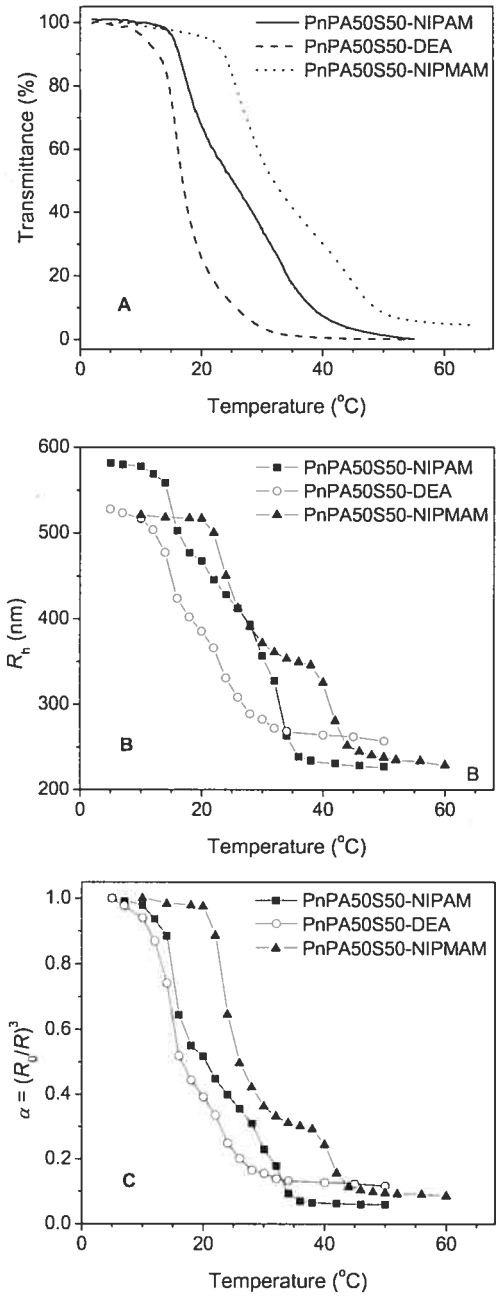

Figure A4. Optical transmittance (A), hydrodynamic diameter R_h (B) and swelling ratio (C, $\alpha = (R_0/R_h)^3$) of doubly thermosensitive core-shell miscrospheres (PnPA50S50 derivatives) as a function of temperature.

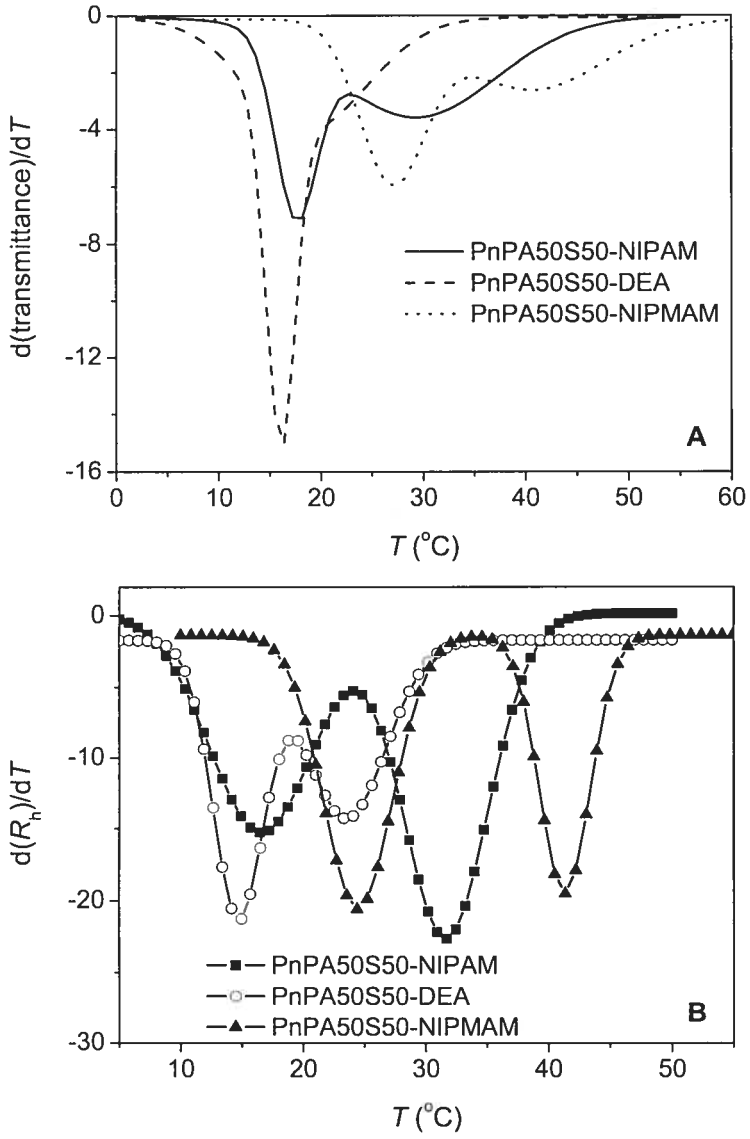

Figure A5. The differentiating curves of data in Figure A4(A) and A4(B).

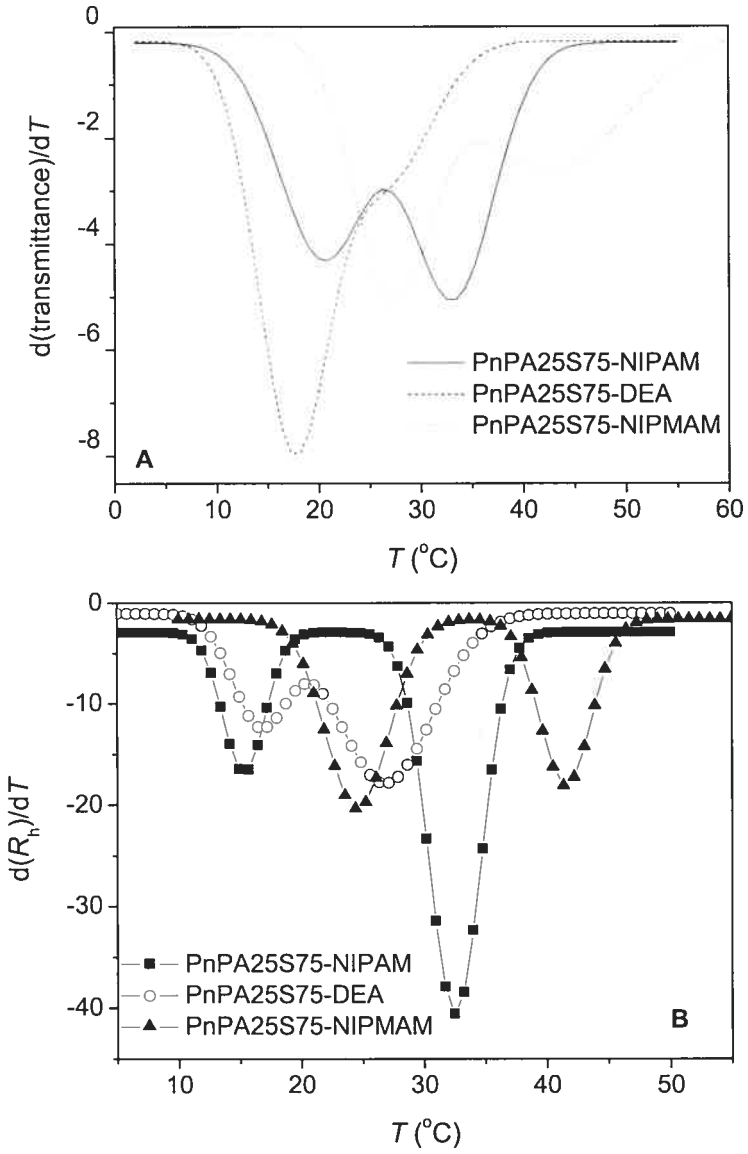

Figure A6. The differentiating curves of data in Figure 3.2(B) and 3.4(B).

C. Appendix of Chapter 4

^{1}H NMR spectrum of DEA

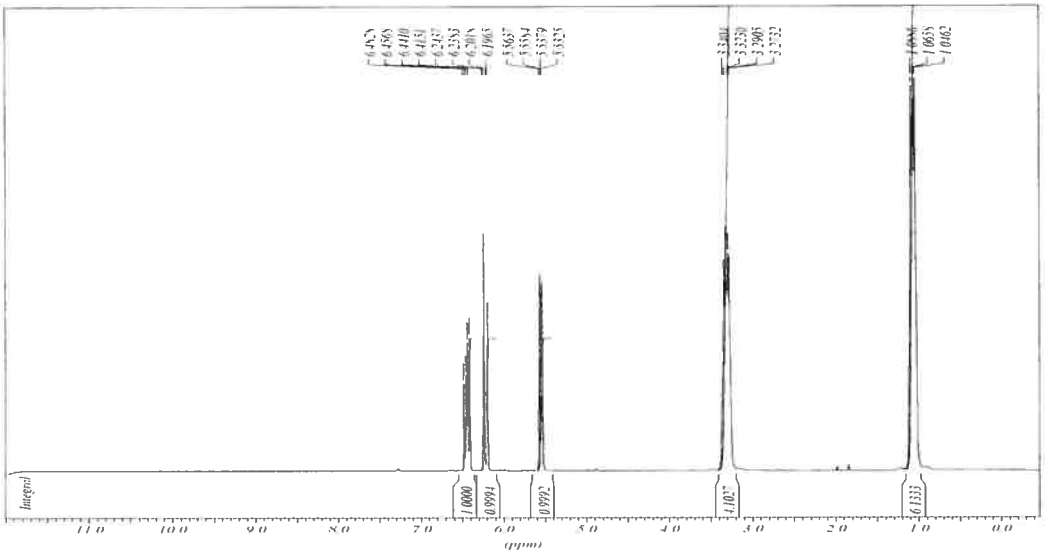

^{1}H NMR spectrum of EA

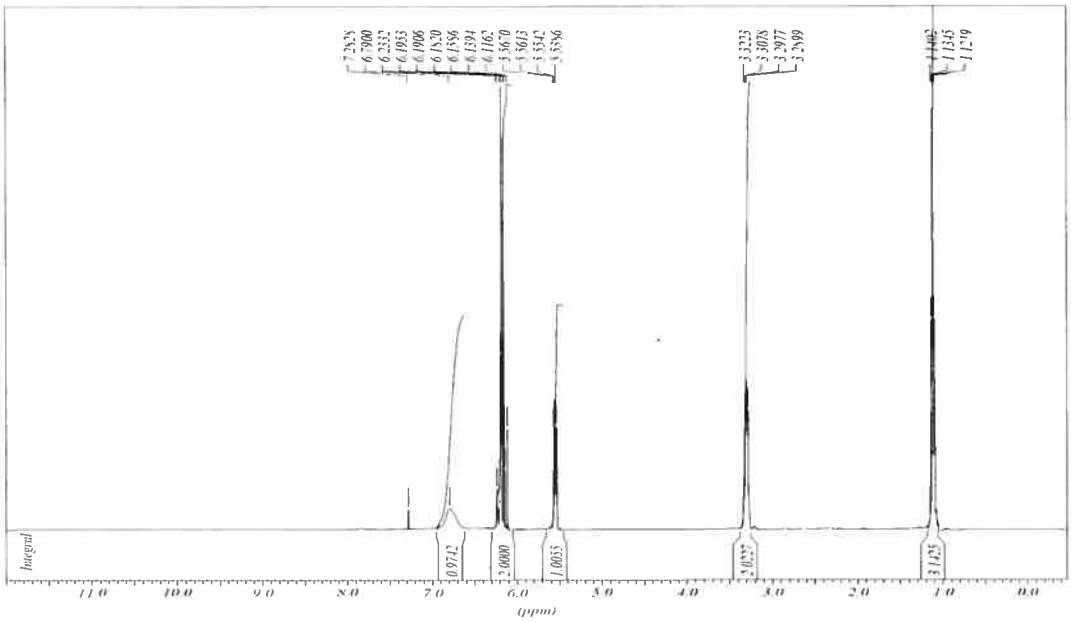

^{1}H NMR spectrum of NAS

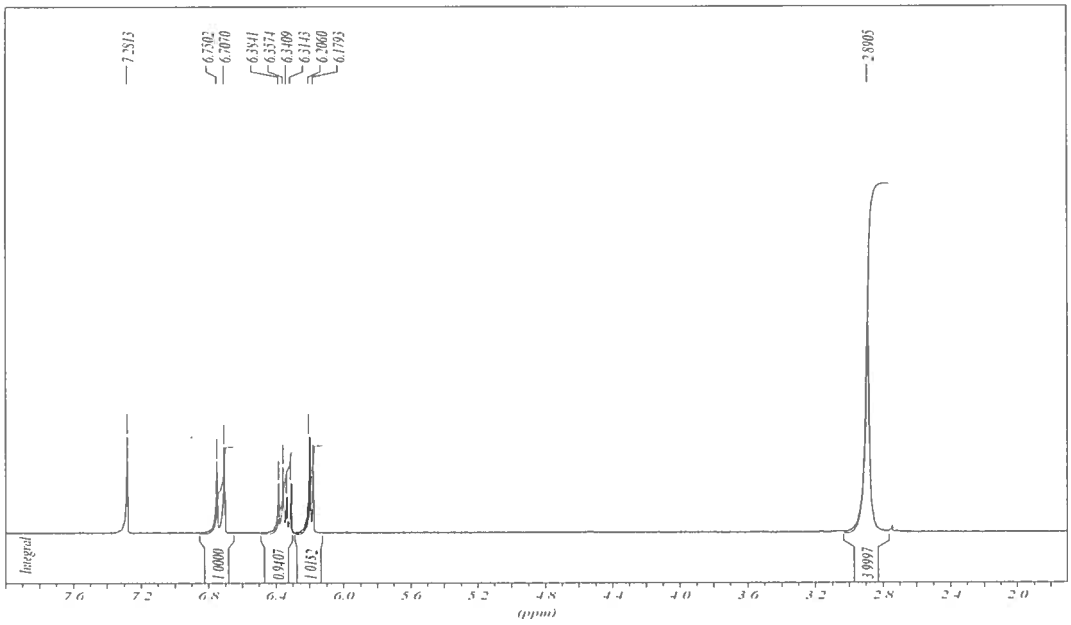

^{13}C NMR spectrum of NAS